iScience

CellPress
OPEN ACCESS

Article

An early glycolysis burst in microglia regulates mitochondrial dysfunction in oligodendrocytes under neuroinflammation

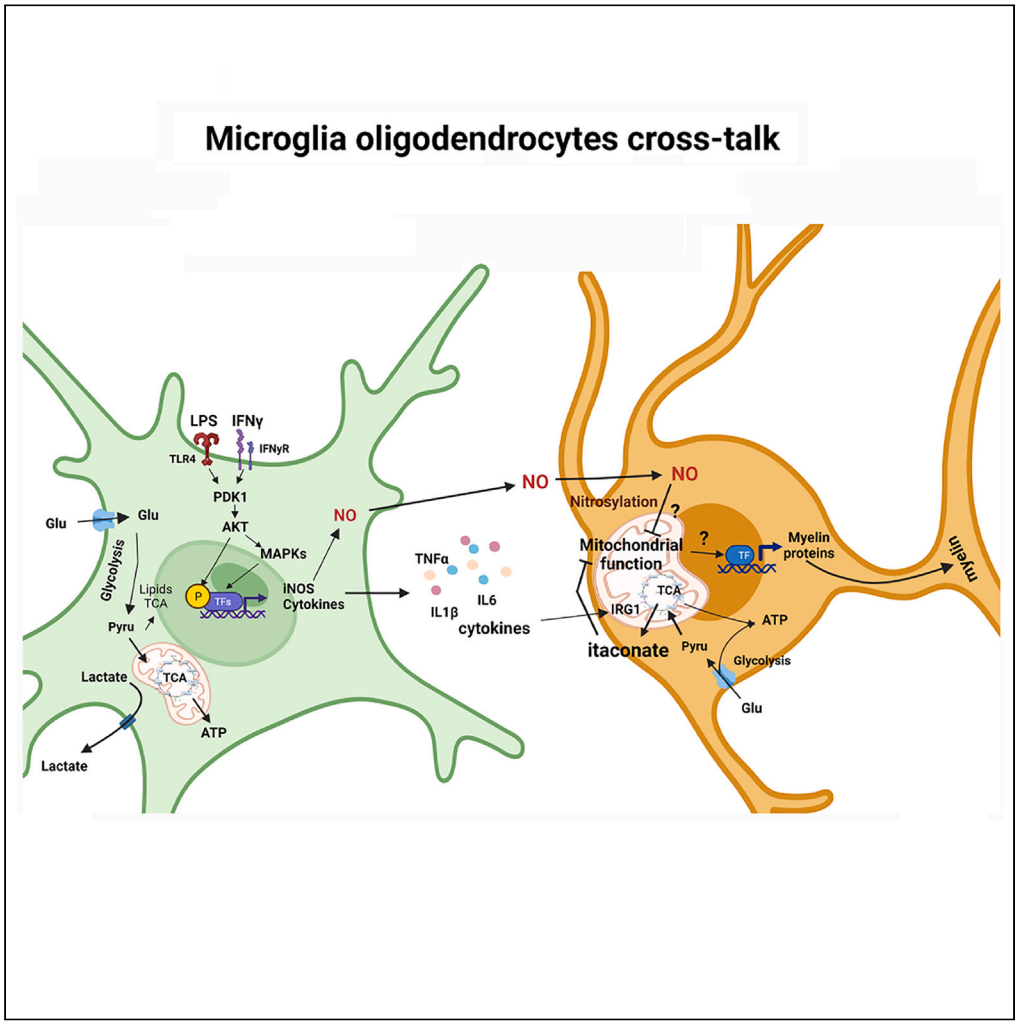

Hamid Suhail, Mohammad Nematullah, Faraz Rashid, ..., Nasrul Hoda, Ramandeep Rattan, Shailendra Giri

sgiri1@hfhs.org

Highlights

Inflammation induced metabolic dysregulation in microglia and oligodendrocytes

PDPK1-AKT signaling facilitated the early burst of glycolysis in activated microglia

Targeting early glycolysis in microglia restored respiration in oligodendrocyte

Microglia-produced NO and itaconate, caused respiration failure in oligodendrocyte

Suhail et al., iScience 26, 107921
October 20, 2023
https://doi.org/10.1016/j.isci.2023.107921

iScience

CellPress
OPEN ACCESS

Article

An early glycolysis burst in microglia regulates mitochondrial dysfunction in oligodendrocytes under neuroinflammation

Hamid Suhail,[1,4] Mohammad Nematullah,[1,4] Faraz Rashid,[1] Mir Sajad,[1] Mena Fatma,[1] Jaspreet Singh,[1] Insha Zahoor,[1] Wing Lee Cheung,[1] Nivedita Tiwari,[1] Kameshwar Ayasolla,[1] Ashok Kumar,[2] Nasrul Hoda,[1] Ramandeep Rattan,[3] and Shailendra Giri[1,5,*]

SUMMARY

Metabolism and energy processes governing oligodendrocyte function during neuroinflammatory disease are of great interest. However, how varied cellular environments affect oligodendrocyte activity during neuroinflammation is unknown. We demonstrate that activated microglial energy metabolism controls oligodendrocyte mitochondrial respiration and activity. Lipopolysaccharide/interferon gamma promote glycolysis and decrease mitochondrial respiration and myelin protein synthesis in rat brain glial cells. Enriched microglia showed an early burst in glycolysis. In microglia-conditioned medium, oligodendrocytes did not respire and expressed less myelin. SCENITH revealed metabolic derangement in microglia and O4-positive oligodendrocytes in endotoxemia and experimental autoimmune encephalitogenic models. The early burst of glycolysis in microglia was mediated by PDPK1 and protein kinase B/AKT signaling. We found that microglia-produced NO and itaconate, a tricarboxylic acid bifurcated metabolite, reduced mitochondrial respiration in oligodendrocytes. During inflammation, we discovered a signaling pathway in microglia that could be used as a therapeutic target to restore mitochondrial function in oligodendrocytes and induce remyelination.

INTRODUCTION

Neuroinflammation is a pathological feature of numerous neurodegenerative diseases, such as multiple sclerosis (MS), Alzheimer's disease (AD), Parkinson disease (PD), Huntington's diseases (HD) and neuropsychiatric disorders.[1–3] It is characterized by lymphocyte/macrophage infiltration, microglial activation, increased chemokine and cytokine production, malfunction of oligodendrocytes, and axonal loss.[4] Brain glial cells have numerous crucial roles, including control of homeostatic activities, myelination, synaptic functions, and transmission of nerve signal.[5,6] In recent years, it has become increasingly apparent that glia-glia crosstalk is critical for brain function during development and disease progression. Microglia are the primary glial cell mediators of neuroinflammatory processes and the first to respond to tissue injury in the CNS. Activated microglia create neurotoxic neuroinflammatory cytokines and reactive oxygen/nitrogen species and release neurotoxic excitatory amino acids.[7] Additionally, they may become reparative by promoting the production of anti-inflammatory cytokines, neuroprotective proteins, and proangiogenic factors. It has been observed that proinflammatory cytokines and mediators, such as nitric oxide (TNFα, IL1β, and NO), are harmful to oligodendrocytes,[8,9] although the underlying mechanism remains unknown.

Mitochondrial dysfunction is a common thread in many neurological diseases, including MS. The majority of studies in postmortem MS brain and preclinical models, including experimental autoimmune encephalomyelitis (EAE), have focused exclusively on the neurons, demonstrating that defective mitochondria contribute to axonal degeneration and neuronal loss, as well as disease progression and irreversible functional impairment.[10–14] The role of mitochondrial dysfunction in oligodendrocytes in MS pathology is underappreciated, despite the fact that oligodendrocytes,[12] rather than axons, have a defect in complex IV of the mitochondrial respiratory chain in MS lesions. Neuroinflammatory processes, as well as mitochondrial dysfunction, increase the production of reactive nitrogen species (RNS) and reactive oxygen species (ROS), resulting in nitrosative stress. Together, these cause metabolic reprogramming in neurons and oligodendrocytes, making them vulnerable to cellular damage or cell death. However, the mechanism of mitochondrial dysfunction in oligodendrocytes during

[1]Department of Neurology, Henry Ford Health System, Detroit, MI 48202, USA
[2]Department of Ophthalmology/Kresge Eye Institute, Department of Anatomy and Cell Biology, Department of Immunology and Microbiology, Wayne State University, Detroit, MI, USA
[3]Division of Gynecology Oncology, Department of Women's Health Services, Henry Ford Health System, Detroit, MI 48202, USA
[4]These authors contributed equally
[5]Lead contact
*Correspondence: sgiri1@hfhs.org
https://doi.org/10.1016/j.isci.2023.107921

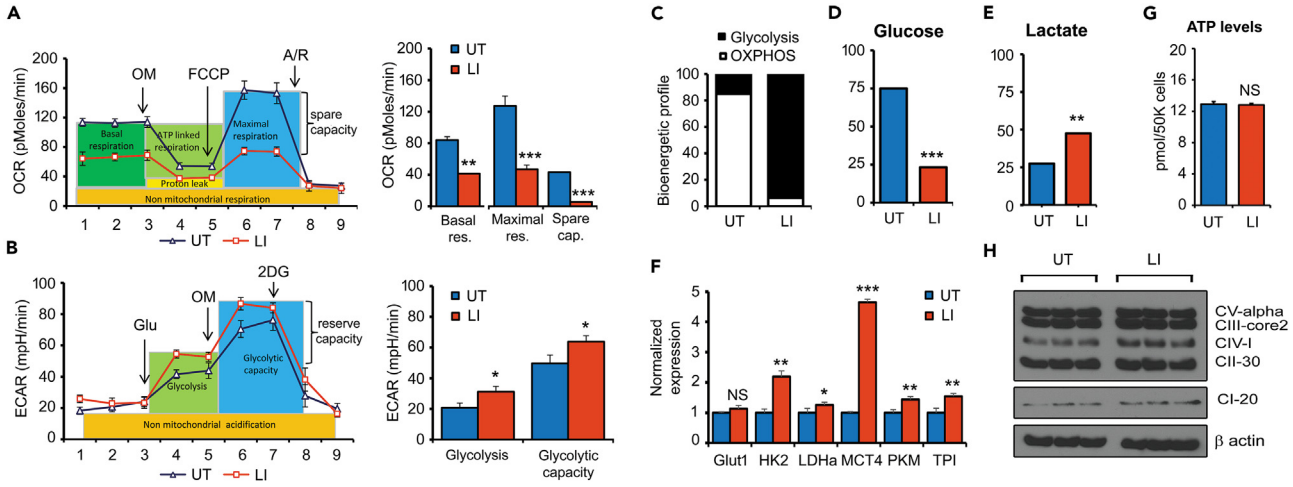

Figure 1. Inflammation reprogramed the bioenergetic phenotype of rat primary mixed glial cells

(A) Oxygen consumption rate (OCR) at basal respiration, maximal respiration, and spare capacity in LPS and IFNγ treated (0.5 μg and 10 ng/mL, respectively; LI-treated) or untreated rat mixed glial cells.

(B) Extracellular acidification rate (ECAR) depicting basal glycolysis, glycolytic capacity and glycolytic reserve capacity in LI-treated or untreated rat mixed glial cells.

(C) Bioenergetic organization of LI-treated or untreated rat mixed glial cells. (N = 4).

(D) Glucose levels in the cell media after treating rat mixed glial cells with or without LI for 24 h (N = 4).

(E) Lactate levels in the cell media after treating rat mixed glial cells with or without LI for 24 h (N = 4).

(F) Glycolytic gene (Glut 1, HK2, LDHa, MCT4, PKM and TPI) expression, normalized with ribosomal protein L27, in rat mixed glial cells after 24 h of LI stimulation (n = 4). Glucose transporter 1 (Glut 1), Hexokinase 2: HK2, Lactate dehydrogenase A: LDHa, Monocarboxylate transporter 4: MCT4, Pyruvate kinase M: PKM, Triosephosphate isomerase: TPI.

(G) Total cellular ATP levels in rat mixed glial cells with or without LI for 24 h (N = 4).

(H) Immunoblot analysis of mitochondrial complexes in rat primary mixed glial cells with or without LI for 24 h. Blot is a presentation of two independent blots. For (A–F), data are shown as mean ± SD. p values were calculated using a one-way ANOVA compared to control conditioned media (CM) groups.

inflammation is less understood, and the role of other co-inhabiting glial cells especially primarily microglia in this phenomenon is poorly understood.

Furthermore, the metabolic changes in activated microglia and their role in exacerbating inflammation and oligodendrocyte dysfunction are relatively unknown. Understanding the crosstalk between microglia and oligodendrocytes during pathological conditions may lead to the identification of signal targets for therapy and the protection of oligodendrocytes to preserve myelination and hence neuronal communication. According to our findings, microglia, not astrocytes, are the key players in causing mitochondrial failure in oligodendrocytes. In this study, we identified a pathological signaling cascade in microglia, PDPK1-AKT-glycolysis, that is responsible for mitochondrial dysfunction and inhibition of the myelin gene expression in oligodendrocytes. Moreover, targeted metabolomics found a higher levels of itaconate, a mitochondrial bifurcated TCA metabolite that could impair mitochondrial function by inhibiting SDH activity in CM-LI treated oligodendrocytes. Our findings shed light on the mechanism of metabolically controlled inflammation in microglia and its impact on oligodendrocyte function, identifying targets for early therapeutic intervention to halt the progression of neuroinflammatory demyelinating diseases like MS.

RESULTS

Bioenergetic changes were caused in primary glial cells by lipopolysaccharide and interferon gamma treatment

We treated primary rat mixed glial cells with lipopolysaccharide plus interferon gamma (LPS and IFNγ; LI) to create an inflammatory environment to investigate the inflammatory signaling events leading to mitochondrial failure in oligodendrocytes and responsible for the reduction of myelin gene expression. Using the Seahorse bioanalyzer, we investigated the bioenergetic state of the cells. Mixed glial cells showed a significant reduction in mitochondrial respiration measured as oxygen consumption rate (OCR) after 24 h of LI treatment, as evidenced by a decrease in basal respiration, maximal respiration, and spare capacity compared to untreated cells (Figure 1A). We also noticed an increase in glycolysis and glycolytic capacity, as measured by extracellular acidification rate (ECAR) (Figure 1B). The bioenergetic organization of the mixed glial cells revealed that untreated cells were primarily reliant on mitochondrial respiration. In contrast, during inflammation, cells rely heavily on glycolysis (Figure 1C). Increased glycolysis in LI-treated cells was also accompanied by increased glucose uptake, lactate production, and glycolytic gene expression (Figures 1D–1F). There was no change in ATP levels, implying that increased glycolysis produces an equivalent amount of ATP to replace and compensate for the loss of mitochondrial respiration (Figure 1G). The reduction in mitochondrial respiration in LI-treated mixed glial cells was not due to mitochondrial loss, as no difference in mitochondrial subunit complex expression was observed in untreated vs. LI-treated mixed glial cells (Figure 1H). In glial cell culture, the metabolic rearrangement caused by LI treatment was

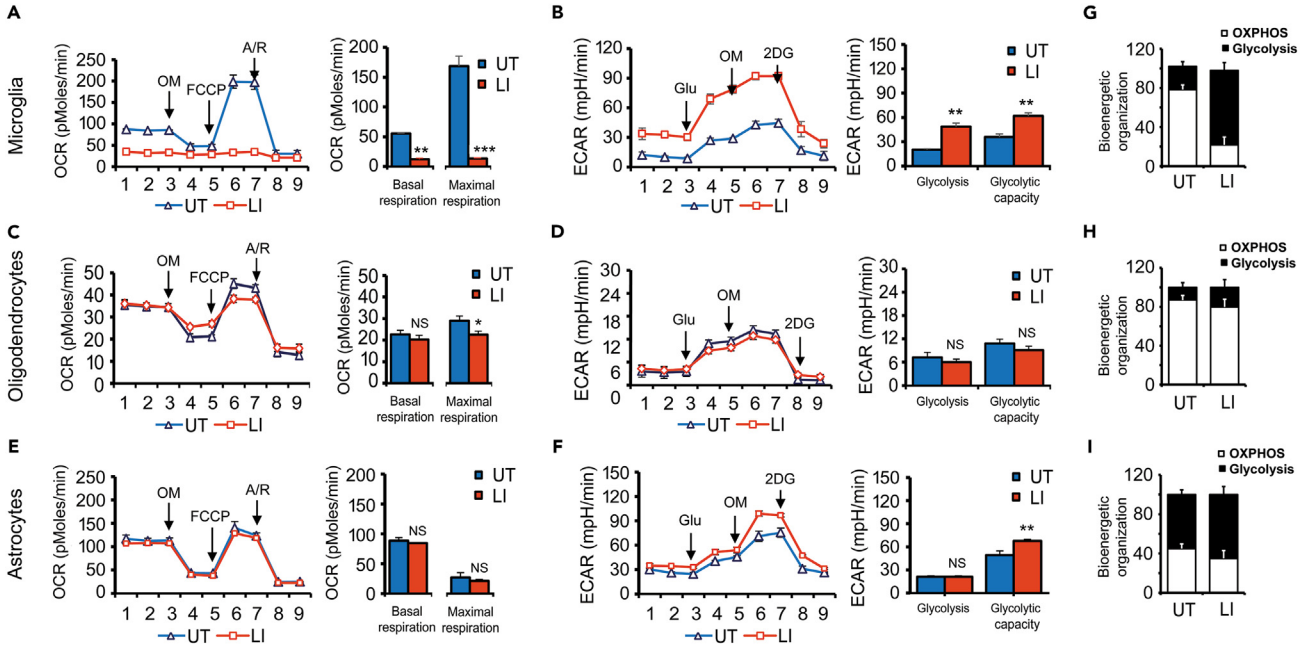

Figure 2. Bioenergetic changes were confined to microglia under inflammatory conditions

(A, C, and E) Oxygen consumption rate (OCR) at basal respiration, ATP-linked, maximal respiration, spare capacity, and proton leak in enriched (A) microglia, (C) oligodendrocytes or (E) astrocytes treated or untreated with LI for 24 h.

(B, D, and F) Extracellular acidification rate (ECAR) depicting basal glycolysis, glycolytic capacity and glycolytic reserve capacity in enriched (B) microglia, (D) oligodendrocytes or (F) astrocytes treated or untreated with LI for 24 h.

(G, H, and I) Bioenergetic organization of LI-treated or untreated in enriched (G) microglia, (H) oligodendrocytes or (I) astrocytes treated or untreated with LI for 24 h. (N = 4).

For (A–F), data are shown as mean ± SD. p values were calculated using a one-way ANOVA compared to control conditioned media (CM) groups.

accompanied by increased expression of proinflammatory cytokines (IL1β, IL6, MIP2, and TNFα) and decreased myelin protein expression including myelin basic protein (MBP), proteolipid protein (PLP), and myelin oligodendrocyte glycoprotein (MOG) without affecting cellular ATP levels (Figures S1A and S1B) (Figure 1G). Overall, our findings show that when exposed to inflammatory conditions, mixed glial cells shift their metabolic demand from mitochondrial respiration to glycolysis to maintain cellular energy levels.

Alteration in bioenergetics were mainly observed in microglia under inflammatory condition

Primary mixed glial culture is composed of many cell types, including astrocytes, microglia, and oligodendrocytes. We enriched primary microglia, oligodendrocyte, and astrocyte cultures with the highest purity (>92 percent) from primary mixed culture to further identify which cell type is primarily undergoing the metabolic shift. The enriched cells were treated with LI for 24 h before being subjected to bioenergetic measurements as before. Similar to macrophages and monocytic dendritic cells,[15,16] microglia showed a complete collapse of mitochondrial respiration with significant induction of glycolysis (Figures 2A and 2B). Oligodendrocytes had a slight decrease in mitochondrial respiration but had no effect on glycolysis (Figures 2C and 2D). Surprisingly, there was no change in mitochondrial function in enriched primary astrocytes. However, compared to untreated cells, LI-treated astrocytes had a slight increase in spare capacity without affecting their basal glycolysis (Figures 2E and 2F). The altered dependency on glycolysis vs. mitochondrial respiration (Figure 2G) and decreased glucose levels and increased lactate in media with significantly higher expression of glycolytic genes indicate a change in the bioenergetic organization of microglia with LI treatment (Figures S2A–S2C). However, no significant differences in bioenergetic organization were observed in oligodendrocytes and astrocytes in response to LI treatment (Figures 2H and 2I). These findings suggest that microglia are the primary cells undergoing altered bioenergetics and acquiring a glycolytic phenotype in the brain mixed glial cell populations, as opposed to astrocytes and oligodendrocytes. Microglia are the most common inflammatory cells in the CNS and plays a key role in neuroinflammatory diseases.[17,18] LI treatment increased glycolysis while also increasing the expression of proinflammatory cytokines and an inflammatory mediator (iNOS) in primary microglia (Figure S2D).

Oligodendrocytes' mitochondrial respiration was attenuated by activated microglial conditioned media (CM)

Because LI treatment reduced the expression of myelin genes in brain mixed glial cells (Figure S1B), we further investigated the functional crosstalk between microglia and oligodendrocytes under inflammatory conditions. Primary enriched microglia were treated with LI for 6 h, followed by three washes with warm serum-free DMEM media to remove unbound LI and replaced with serum-free DMEM media. The

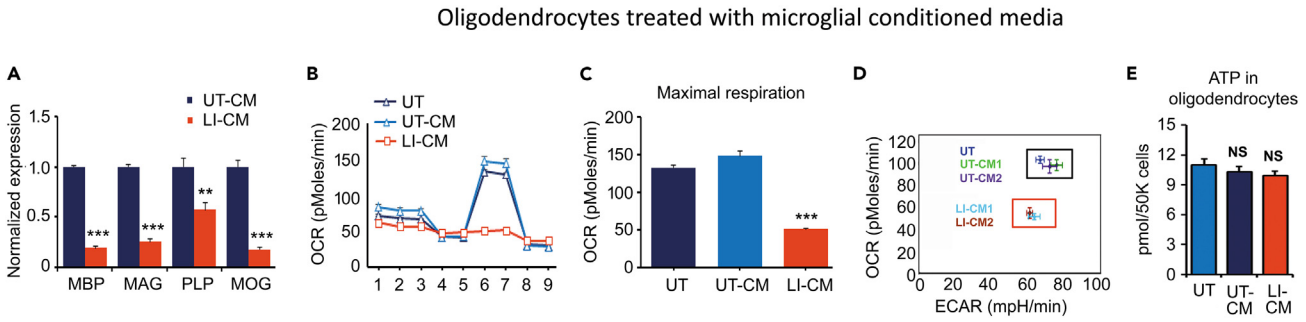

Figure 3. Activated microglial conditioned media (CM) inhibited mitochondrial respiration in oligodendrocytes

(A) The normalized expression for myelin genes in primary oligodendrocytes cultured with microglial LI-conditioned media (LI-CM) or untreated microglia-CM (UT-CM) for 24 h (N = 4). MBP, myelin basic protein; MAG, myelin-associated glycoprotein; PLP, Proteolipid protein; MOG, myelin oligodendrocyte glycoprotein.

(B and C) OCR in primary oligodendrocytes at 24 h cultured with microglial LI-CM or UT-CM. Maximal respiration rate presented as a bar graph (N = 6).

(D) Bioenergetic state of the primary oligodendrocytes at 24 h cultured with microglial LI-CM or UT-CM. Two independent UT-CM and LI-CM were used to demonstrate the reproducibility of mitochondrial failure in oligodendrocytes.

(E) Total cellular ATP levels examined in primary oligodendrocytes at 24 h cultured with microglial untreated (UT), LI-CM or Ut-CM (N = 4).

For (A, C, and E) data are shown as mean ± SD. p values were calculated using a one-way ANOVA compared to control conditioned media (CM) groups.

serum-free conditioned media (LI-CM) was filtered and plated on primary enriched oligodendrocytes in a 1:3 ratio with serum-free DMEM media after 18 h of incubation. We used LC-MS/MS to rule out the possibility of LPS contamination in CM-LI media used for oligodendrocyte treatment and found no traces of LPS after washing (Figure S3A). The quantitative PCR was used to examine the expression of myelin proteins as a function of oligodendrocytes after 24 h of incubation. The expression of myelin genes was significantly reduced in primary oligodendrocytes cultured with LI-CM compared to untreated conditioned media (UT-CM) from microglia (Figure 3A). Furthermore, the maximal mitochondrial respiration of LI-CM exposed primary oligodendrocytes was significantly reduced than that of UT-CM exposed cells (Figures 3B and 3C), indicating a low-metabolic oligodendrocyte phenotype (Figure 3D). Similarly, when cultured with microglia LI-CM, the maximal mitochondrial respiration in the oligodendrocyte cell line B12[19,20] was significantly reduced (Figure S3B). The metabolic and functional changes mediated by microglia in oligodendrocytes had no effect on their survival or total cellular ATP levels (Figure 3E). These findings suggest that under inflammatory conditions, microglia-derived factor(s) are responsible for dampening oligodendrocyte mitochondrial respiration and function, implying a functional crosstalk between microglia and oligodendrocytes. To investigate the relationship between mitochondrial respiration and myelin gene expression further, oligodendrocytes were treated with oligomycin (100 nM), an ATP synthase inhibitor that blocks its proton channel (F0-subunit). Oligomycin inhibited mitochondrial respiration, which significantly reduced myelin gene expression (Figure S3C) without affecting primary oligodendrocyte survival. Oligodendrocytes rely on mitochondrial respiration for energy, but the loss of mitochondrial function had no effect on cellular ATP levels (Figures 3E and S4A), indicating that mitochondrial respiration is important for oligodendrocyte function but not for survival under inflammatory conditions. We investigated whether glycolysis could be upregulated as a compensatory mechanism in oligodendrocytes to meet their energy needs. Primary rat oligodendrocytes and the B12 oligodendrocyte cell line displayed significantly higher glycolysis under similar LI-CM exposure conditions (Figures S4B and S4C). LI-CM treated primary oligodendrocytes and B12 cell line showed increased glucose uptake and altered bioenergetic organization, respectively (Figures S4D and S4E), indicating that oligodendrocytes undergo metabolic reprogramming to adapt and maintain cellular ATP levels by switching from mitochondrial respiration to glycolysis, most likely to ensure survival.

Metabolic changes in microglia and oligodendrocytes *in vivo*

To examine the *in vivo* relevance of our finding, we used two models such as endotoxemia and experimental autoimmune encephalomyelitis (EAE), a preclinical mouse model of MS. Administration of lipopolysaccharide (LPS), a structural component of gram-negative bacteria, *in vivo* is a well-established experimental model of endotoxemia including (neuro)inflammation and sepsis.[21] To examine the impact of endotoxemia on metabolic changes in microglia and oligodendrocytes, we intraperitoneally injected sublethal dose of LPS (1 mg/kg body weight) and post 6 h, using Percoll, single cell population of brain tissue was prepared and processed for SCENITH (Single Cell ENergetIc metabolism by profiling Translation inHibition), a FACS-based, quantitative analysis of mRNA translation in single cells.[22–24] SCENITH takes advantage of cells being exposed to a short pulse of Puromycin (PURO), which is incorporated in polypeptides that are being translated. Translation being an energy consuming process,[25] SCENITH is a proxy for the metabolic fitness of the cell and its metabolic outcome have been reported to correlate well with Seahorse.[23,24] We found that microglia from endotoxemia group showed higher glycolysis dependency, without affecting mitochondrial respiration (Figure 4A). Under similar experimental condition, we examined the metabolic fitness of pre-oligodendrocytes using their marker; O4 and found that mitochondrial respiration is significantly reduced, however, glycolysis dependency was increased in O4 positive oligodendrocytes in endotoxemia model compared to PBS injected group (Figure 4B). Gating strategy for analyzing metabolic changes in microglia and O4 oligodendrocytes is reported under Figure S5. Another *in vivo* model we used is chronic EAE in B6 mice. We induced EAE disease using MOG_{35-55}, on day 18 post immunization when clinical score was

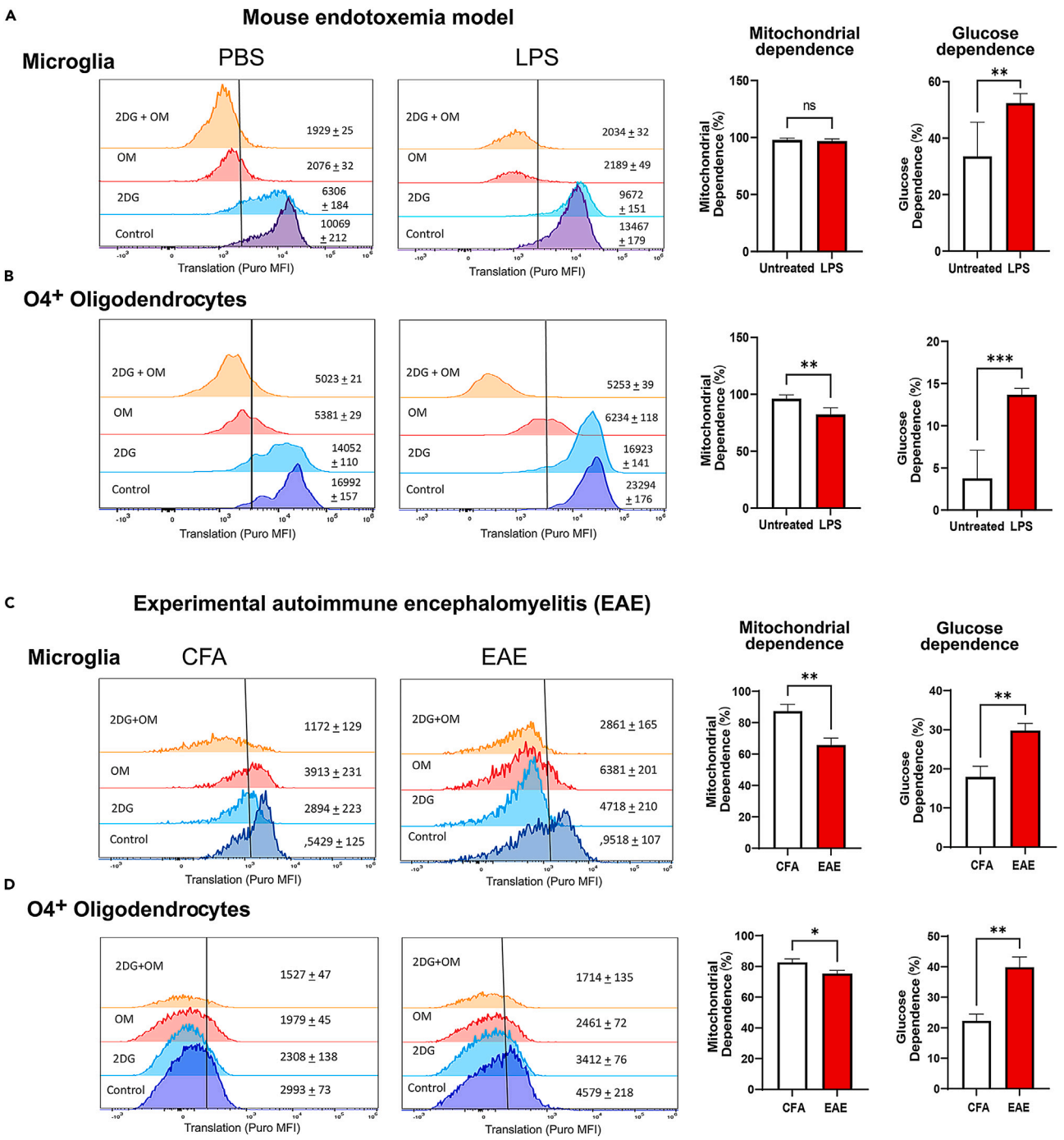

Figure 4. Bioenergetic analysis of microglia and O4 positive oligodendrocytes in endotoxemia and EAE models

(A and B) Puromycin incorporation (MFI values indicated) in microglia ($CD45^{low}CD11b^{+}$) and O4 positive oligodendrocytes ($CD45^{-}CD11b^{-}O4^{+}$) in untreated (saline as vehicle) and LPS treated groups (N = 5). Metabolic changes, including mitochondrial dependence and glucose dependence, in untreated and LPS-treated microglia and O4+ oligodendrocyte populations are depicted as a bar graph (N = 5).

(C and D) Puromycin incorporation (MFI values indicated) in microglia and O4 positive oligodendrocytes in CFA and EAE groups (N = 5) during four different metabolic treatments. Metabolic changes in the populations of microglia and O4+ oligodendrocytes in the CFA and EAE groups are shown as a bar graph (N = 5). The data represent the mean ± standard deviation (SD) of three separate experiments. The values are given as mean ± SD. NS, not significant, *P 0.05, **P 0.01, ***P 0.001, one-way ANOVA compared to untreated or CFA.

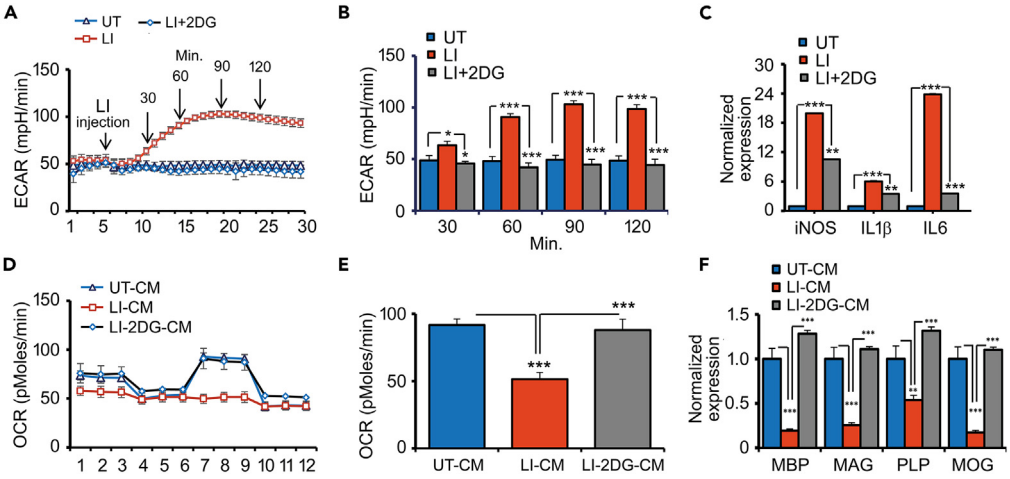

Figure 5. Inhibition of early glycolytic burst in primary microglia reduced inflammation and restored myelin genes expression in oligodendrocytes

(A and B) Real-time measurement of ECAR in primary microglia stimulated with LI in Seahorse bioanalyzer using the second port in the presence or absence of 2DG. Basal ECAR presented as a bar graph at 90 min in primary microglia stimulated with LI in the presence or absence of 2DG (N = 6).

(C) Normalized expression of proinflammatory cytokines (IL1b and IL6) and iNOS in stimulated microglia in the presence and absence of 2DG after 3 h of LI treatment.

(D and E) OCR response in primary oligodendrocytes treated with CM of LI stimulated microglia in the presence and absence of 2DG. Maximal respiration is presented as a bar graph (N = 6).

(F) Expression of myelin genes in oligodendrocytes treated with CM of LI stimulated microglia in the presence and absence of 2DG (N = 4). All data are shown as mean ± SD. p values were calculated using a one-way ANOVA compared to control conditioned media (CM) or LI-2DG-CM groups.

3.1 ± 0.5, single cell population of brain tissue was prepared and processed for SCENITH. We found a significant decrease in mitochondrial dependency in microglia with a significant increase in glycolysis (Figure 4C). A similar observation was found in O4+ oligodendrocytes with increased glycolysis dependency (Figure 4D) suggesting that metabolic derangement in microglia and oligodendrocytes are consistent *in vitro* and *in vivo* models.

Early glycolytic burst in primary microglia caused inflammation and decreased myelin gene expression in primary oligodendrocytes

To examine that the altered oligodendrocyte bioenergetic profile and function are mediated by microglial derived factor(s), which are governed by the enhanced glycolysis induced in stimulated microglia, we studied real-time changes in ECAR and inflammatory mediators in primary microglia. The addition of LI caused a rapid increase in ECAR, indicating the occurrence of an early glycolysis burst in microglia, which was prevented by the glycolytic inhibitor (2-deoxyglucose; 2-DG) (Figures 5A and 5B). 2DG inhibited proinflammatory cytokines (IL1β and IL6) and iNOS expression in microglia by attenuating the early burst of glycolysis (Figure 5C). To investigate whether early glycolytic burst in microglia plays a role in oligodendrocyte mitochondrial dysfunction, primary oligodendrocytes were cultured for 24 h in the presence of microglial UT-CM, LI-CM, or LI-CM with 2DG (LI-CM-2DG). We found that oligodendrocytes cultured with LI-CM-2DG restored maximal mitochondrial respiration when compared to LI-CM (Figures 5D and 5E), resulting in full recovery of myelin gene expression (Figure 5F). These findings suggest that the early burst of glycolysis in activated microglia plays an important role in the production of proinflammatory mediators, resulting in decreased oligodendrocyte mitochondrial function and myelin gene expression.

The early glycolytic burst in microglia and the expression of myelin genes in oligodendrocytes are controlled by PDPK1/Akt signaling, an upstream event under inflammatory condition

TLR4-dependent activation of PI3K-protein kinase B/AKT signaling is required for the inflammatory cascade in microglia/macrophages, and PDPK1 mediates PI3K-induced activation of AKT.[26] LI treatment activates PDPK1 and AKT in primary microglia as early as 5 min after treatment, as evidenced by increased phosphorylation of PDPK1 and AKT1 in a time-dependent manner (Figure 6A). To investigate the role of PDPK1 and AKT in the increase in early glycolysis observed in microglia during inflammation, we used BX795 and API-1 to inhibit their activity (will be referred to as iPDPK1 and iAKT, respectively) (Figure 6B). In primary microglia, inhibiting PDPK1 and AKT activity eliminated the LI-induced early glycolysis burst as well as the expression of proinflammatory cytokines and iNOS genes (Figures 6C–6E). When oligodendrocytes were cultured in microglial LI-CM with or without these inhibitors (CM-iPDPK1 or CM-iAKT), CM with inhibitors restored maximal mitochondrial respiration (Figures 6F and 6G) that was inhibited in the presence of LI-CM and restored myelin gene expression (Figure 6H). The bioenergetic organization predicts that untreated primary oligodendrocytes rely on both glycolysis and mitochondrial respiration for

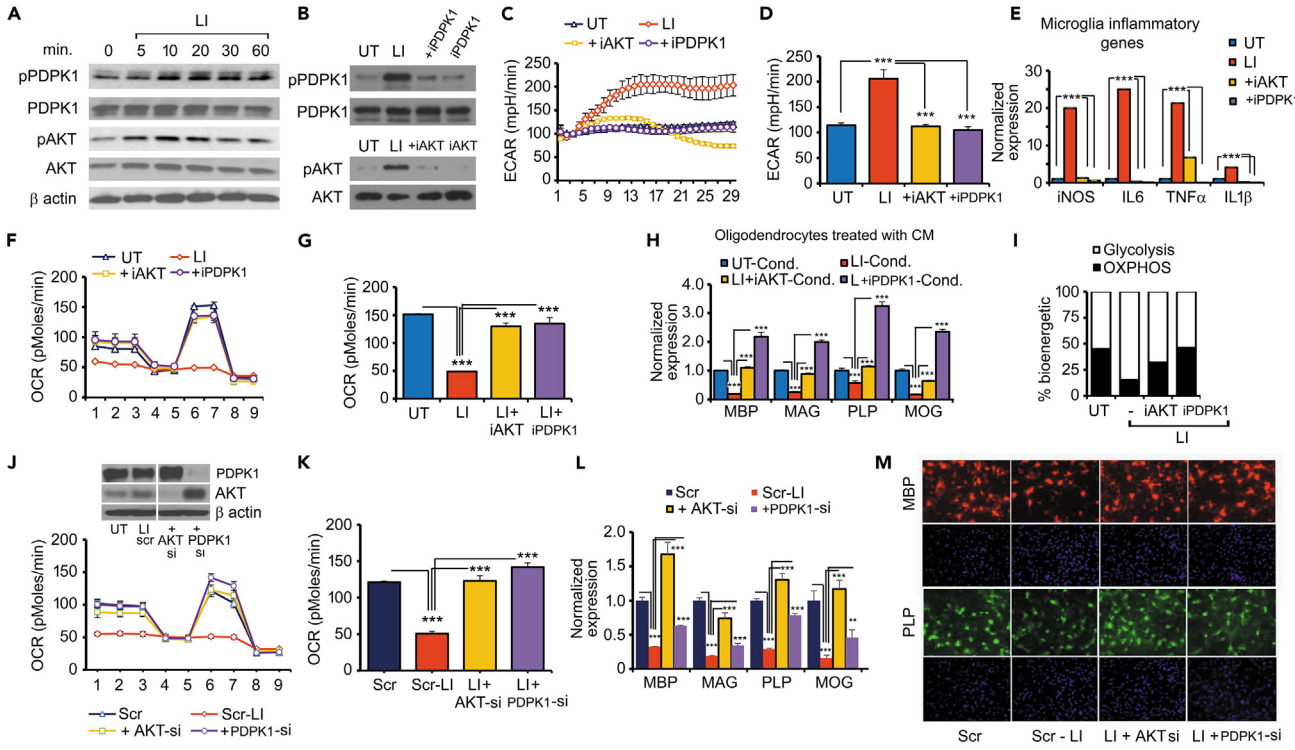

Figure 6. PDPK1/Akt signaling is an upstream event regulating an early glycolytic burst in microglia and myelin genes expression in oligodendrocytes

(A) Time course of PDPK1 and AKT activation (phosphorylation status) in response to LI in primary microglia. Blot is a representation of two independent experiments.

(B) PDPK1 (BX795) and AKT (API-1) inhibitors attenuated activation of PDPK1 and AKT phosphorylation in activated primary microglia. Blot is a representation of two independent experiments.

(C) Real time measurement of ECAR in primary microglia stimulated with LI in Seahorse bioanalyzer using the second port in the presence or absence of PDPK1 or AKT inhibitors (N = 6).

(D) ECAR presented as a bar graph at 60 min in primary microglia stimulated with LI in the presence or absence of PDPK1 or AKT inhibitors (N = 6).

(E) Normalized expression of proinflammatory cytokines (IL1β, IL6, and TNFα) and iNOS in stimulated microglia in the presence and absence of PDPK1 or AKT inhibitors after 3 h of LI treatment (N = 4).

(F and G) OCR in primary oligodendrocytes treated with CM of LI stimulated microglia conditioned media (CM) in the presence and absence of PDPK1 or AKT inhibitors post 24 h culture. Maximal respiration is presented as a bar graph (N = 6).

(H) Expression of myelin genes in oligodendrocytes treated with CM of LI stimulated microglia conditioned media (CM) in the presence and absence of PDPK1 or AKT inhibitors (N = 4).

(I) Bioenergetic organization of enriched oligodendrocyte cultured with CM of LI stimulated microglia conditioned media (CM) in the presence and absence of PDPK1 or AKT inhibitors for 24 h (N = 6).

(J and K) OCR in primary oligodendrocytes treated with CM of LI stimulated microglia conditioned media (CM) in siRNA-lentivirus mediated downregulation of PDPK1 or AKT (N = 6). Immunoblot analysis of downregulated PDPK1 and AKT expression in siRNA lentivirus induced transduction in microglia. Maximal respiration is presented as a bar graph (N = 6).

(L) Expression of myelin genes in oligodendrocytes treated with CM of LI stimulated microglia conditioned media (CM) in siRNA-lentivirus mediated downregulation of PDPK1 or AKT (N = 4).

(M) Immunocytochemistry of MBP and PLP in siRNA-lentivirus mediated downregulation of PDPK1 or AKT in microglia in the presence or absence of LI. The picture is representative of two independent experiments.

For (C–L), data are shown as mean ± SD. p values were calculated using a one-way ANOVA compared to control conditioned media (CM) or LI-inhibitors-CM groups.

cellular ATP maintenance; however, when oligodendrocytes were cultured with LI-CM, oligodendrocytes rely primarily on glycolysis as a power generator due to mitochondrial respiration failure. Co-culturing oligodendrocytes in CM-iPDPK1 or CM-iAKT restored mitochondrial respiration, allowing oligodendrocytes to regain bioenergetic organization similar to untreated cells (Figure 6I). We used siRNA to downregulate the expression of PDPK1 and AKT in primary microglia to support this observation (Figure 6J). LI-AKT-si or LI-PDPK1-si conditioned media of downregulated PDPK1 or AKT in microglia restored the LI-CM-induced mitochondrial dysfunction (Figure 6K) and restored myelin genes in primary oligodendrocytes (Figures 6L and 6 M). The pharmacological and siRNA approaches identified PDPK1 and AKT as upstream regulators of the early glycolysis burst in microglia, which leads to a cascade of disruptive oligodendrocyte energetics and function. Thus,

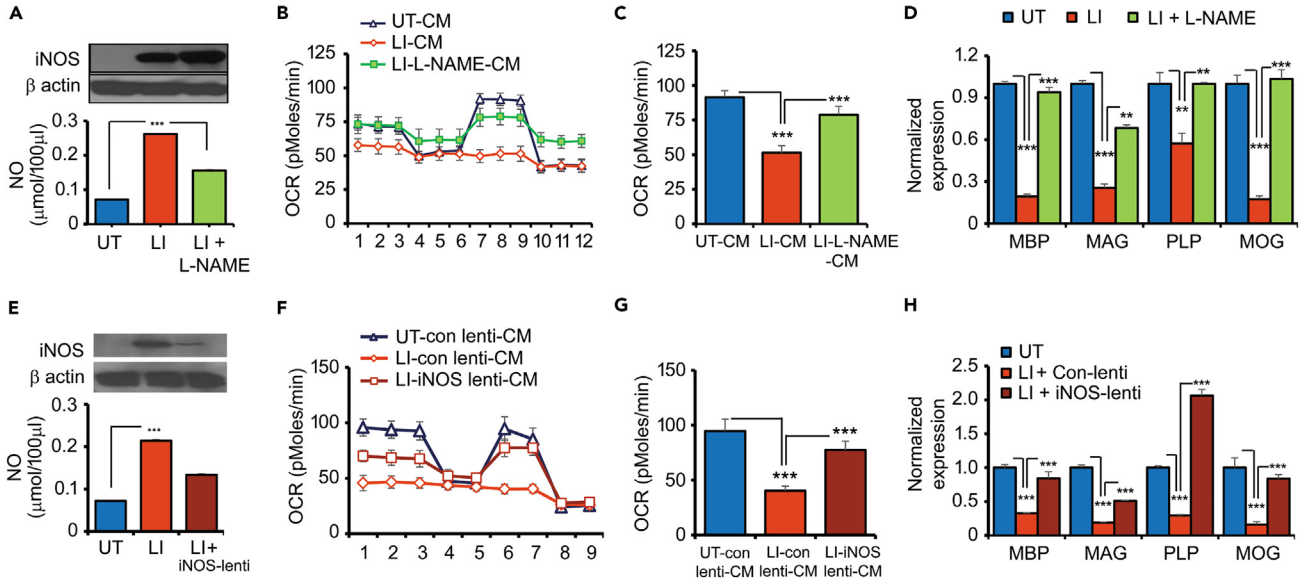

Figure 7. Microglia-driven NO, a one of the factors for dysfunction of mitochondrial respiration in oligodendrocytes

(A) Effect of NOS inhibitor (L-NAME; 100 μM) on NO production in primary microglia in response to LI using Griess reagent. Immunoblot analysis of iNOS in the presence or absence of L-NAME in activated microglia. Blot is representative of two independent experiments.

(B and C) OCR in primary oligodendrocytes treated with CM of LI stimulated microglia conditioned media (CM) in the presence and absence of L-NAME post 24 h culture. Maximal respiration is presented as a bar graph (N = 6).

(D) Expression of myelin genes in oligodendrocytes treated with CM of LI stimulated microglia conditioned media (CM) in the presence and absence of L-NAME (N = 4).

(E) Levels of NO in siRNA lentivirus-mediated downregulated iNOS expression in primary microglia in response to LI using Griess reagent (N = 4). Immunoblot analysis of iNOS in siRNA lentivirus-mediated downregulated iNOS expression in primary activated microglia.

(F and G) OCR in primary oligodendrocytes treated with CM of LI stimulated microglia conditioned media (CM) in siRNA-lentivirus mediated downregulation of iNOS. Maximal respiration is presented as a bar graph (N = 6).

(H) Expression of myelin genes in oligodendrocytes treated with CM of LI stimulated microglia conditioned media (CM) in siRNA-lentivirus mediated downregulation of iNOS (N = 4).

For (A–H), data are shown as mean ± SD. p values were calculated using a one-way ANOVA compared to control conditioned media (CM), LI-L-NAME-CM LI-iNOS-lenti-CM groups.

PDPK1 and AKT may be an appealing therapeutic target in microglia to maintain oligodendrocyte mitochondrial function and myelin generation during inflammation.

Nitric oxide (NO) produced by microglia is one of the causes of oligodendrocytes' dysfunctional mitochondrial respiration

Nitric oxide (NO), a signaling molecule, has been linked to a number of physiological and pathological conditions associated with neurodegenerative disorders.[27,28] NO is primarily produced by inducible nitric oxide synthase (iNOS) in microglia during neuroinflammatory disorders.[28] We measured NO levels in the supernatant of LI-treated primary microglial cells and as expected that LI treatment significantly increased NO production and iNOS expression compared to untreated cells (Figure S6A). Furthermore, inhibiting PDPK1 and AKT with specific inhibitors reduced iNOS expression and NO production in LI-treated primary microglial cells (Figure S6B), implying that microglia-driven NO may be a critical factor in mitochondrial failure and oligodendrocyte dysfunction. We used L-NG-Nitroarginine methyl ester (L-NAME), a non-selective NOS inhibitor, to block iNOS activity in activated microglia to see if NO is a key player in the crosstalk between activated microglia and oligodendrocytes. L-NAME treatment had no effect on iNOS expression but significantly reduced NO production in treated microglia (Figure 7A). When compared to LI-CM treatment, conditioned media of primary microglia treated with L-NAME (LI-L-NAME-CM) restored oligodendrocyte mitochondrial function (Figures 7B and 7C). Furthermore, L-NAME treatment prevented LI-CM-mediated loss of myelin gene expression in primary oligodendrocytes (Figure 7D). To confirm this finding, we used shRNA to reduce iNOS expression in primary microglial cells (Santa Cruz Biotech). Transduction of shRNA lentivirus against iNOS reduced iNOS expression and eliminated NO production when compared to the control group of LI treated shRNA lentivirus (Figure 7E). LI-iNOS-lenti-CM (conditioned media of primary microglial cells transduced with shRNA against iNOS lentivirus) restored mitochondrial dysfunction and attenuated myelin gene expression in primary oligodendrocytes caused by treatment with CM of LI treated shRNA lentivirus control group (LI-con-lenti-CM) (Figures 7F–7H). These findings strongly suggest that NO from microglia is causing oligodendrocyte mitochondrial dysfunction during inflammation.

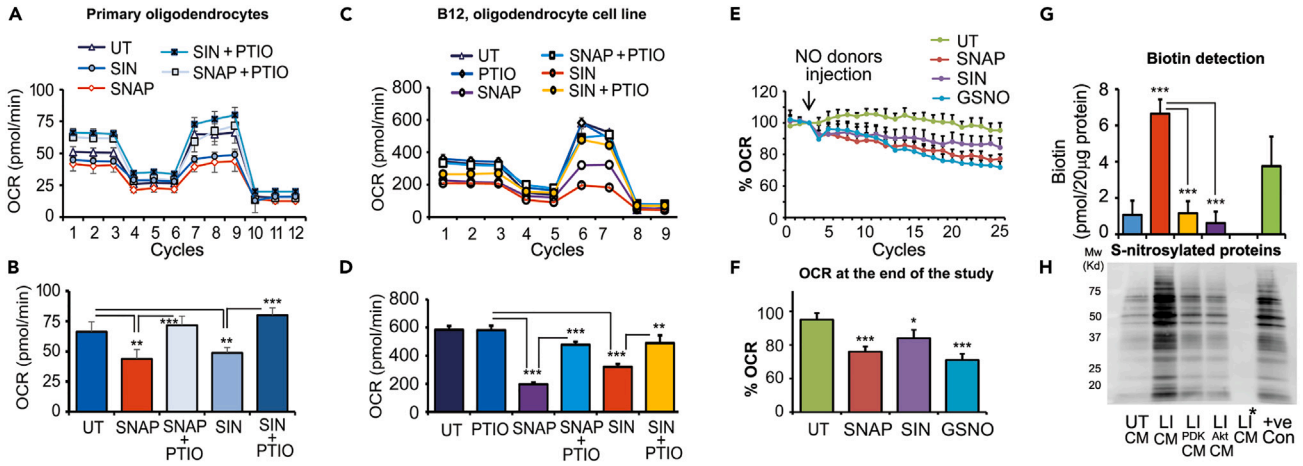

Figure 8. Nitric oxide inactivates mitochondrial function in oligodendrocytes

(A–D) OCR in primary oligodendrocytes (A and B) and B12 oligodendrocyte cell line (C and D) treated with various NO donors (SIN and SNAP) and quencher (PTIO). Maximal respiration is presented as a bar graph (N = 6).

(E and F) Real-time measurement of OCR in primary oligodendrocytes in Seahorse bioanalyzer with various NO donors (SIN, SNAP and GSNO). Maximal respiration is presented as a bar graph (N = 6).

(G and H) Biotin detection and S-nitrosylation of proteins at 24 h of indicated treatment of B12 oligodendrocyte cell line (N = 4). S-nitrosylated blot is representative of two independent experiments.

For (A–G), data are shown as mean ± SD. p values were calculated using a one-way ANOVA compared to control conditioned media (CM), NO donors with or without quencher, LI-iPDK-CM or LI-iAKT-CM groups.

Nitric oxide inactivates mitochondrial function in primary oligodendrocytes

To provide direct evidence, we used NO donors such as 3-morpholinosydnonimine (SIN-1) and S-Nitroso-N-acetylpenicillamine (SNAP) on primary oligodendrocytes, which significantly reduced mitochondrial respiration (Figures 8A–8D). NO scavenger (α-Phenyltetramethylnitronyl nitroxide; PTIO) restored the NO donors-mediated abrogation of mitochondrial function in primary oligodendrocytes and the rat B12 oligodendrocyte cell line (Figures 8A–8D). In primary oligodendrocyte culture, the addition of various NO donors inactivates mitochondrial respiration in real time (Figures 8E and 8F), providing direct evidence of NO-mediated mitochondrial dysfunction in oligodendrocytes. Culturing primary oligodendrocytes with microglia LI-CM increased biotinylation and S-nitrosylation, which was reduced by PDPK1 and AKT inhibitors (Figures 8G and 8H). Given the fact that nitrosylation mediated inhibition of mitochondrial complex 1,[29,30] our data suggest that NO-driven from microglia is one of the factor for mitochondrial dysfunction of oligodendrocytes.

Itaconate production is induced in oligodendrocytes treated with CM-LI

We further performed a targeted glycolysis-TCA metabolomics study to better understand the metabolic reprograming of oligodendrocytes treated with CM-LI. Several glycolysis-TCA cycle metabolites, including sedohepulose-7-phosphate (SH7P), citrate, and succinate, were significantly increased in CM-LI treated oligodendrocytes compared to CM-treated oligodendrocytes, as shown in Figure 9A. The isotopomer and isotopologue distribution of metabolites derived from uniformly labeled [U-^{13}C]-Glc (glucose) metabolism in oligodendrocytes cultured with UT-CM or LI-CM was determined using a stable isotope-resolved metabolomics (SIRM) approach. As expected, there is a significant increase in several glycolytic metabolites enriched in ^{13}C derived from labeled glucose, such as SH7P, 2PG-3PG, PEP, and lactate (Figure 9B), implying that glucose metabolism is enhanced, possibly compensating for energy lost due to mitochondrial dysfunction. There was no significant change in the ratio of NAD+/NADH (Figure 9B) or steady-state ATP levels (Figure 3E) in CM-LI treated oligodendrocytes, indicating that treated oligodendrocytes were able to maintain cellular energy in cells despite mitochondrial dysfunction. Itaconate, a bifurcated TCA metabolite, was found to be significantly higher in CM-LI-treated oligodendrocytes (Figure 9A). Its increased production is due to glycolysis, as enriched C13-itaconate levels are significantly elevated in CM-LI treated oligodendrocytes compared to CM-treated oligodendrocytes (Figure 9B). Itaconate is a mitochondrial-selective metabolite produced by immune responsive gene 1 (*Irg*1, also known as ACOD1)[31] from the decarboxylation of TCA cycle intermediate *cis*-aconitate. *Irg*1 RNA and protein expression is increased in CM-LI treated oligodendrocytes, resulting in elevated levels of itaconate (Figures 9C–9E). Itaconate is an innate immune metabolite specifically produced in stimulated immune cells.[32,33] There are no study reporting the production of itaconate in oligodendrocytes under inflammatory condition, therefore, we examine its levels in oligodendrocyte under inflammatory conditions using LI and we found that direct treatment of oligodendrocyte with LI induced the expression of *Irg*1 at protein level along with intracellular itaconate levels (Figures S7A and S7B), supporting the increased levels of itaconate in oligodendrocyte under inflammatory conditions. The expression of *Irg*1 at mRNA and protein and itaconate levels are also induced significantly in primary microglia (Figure S7C–S7Ei), raising the possibility if elevated itaconate in CM-LI treated

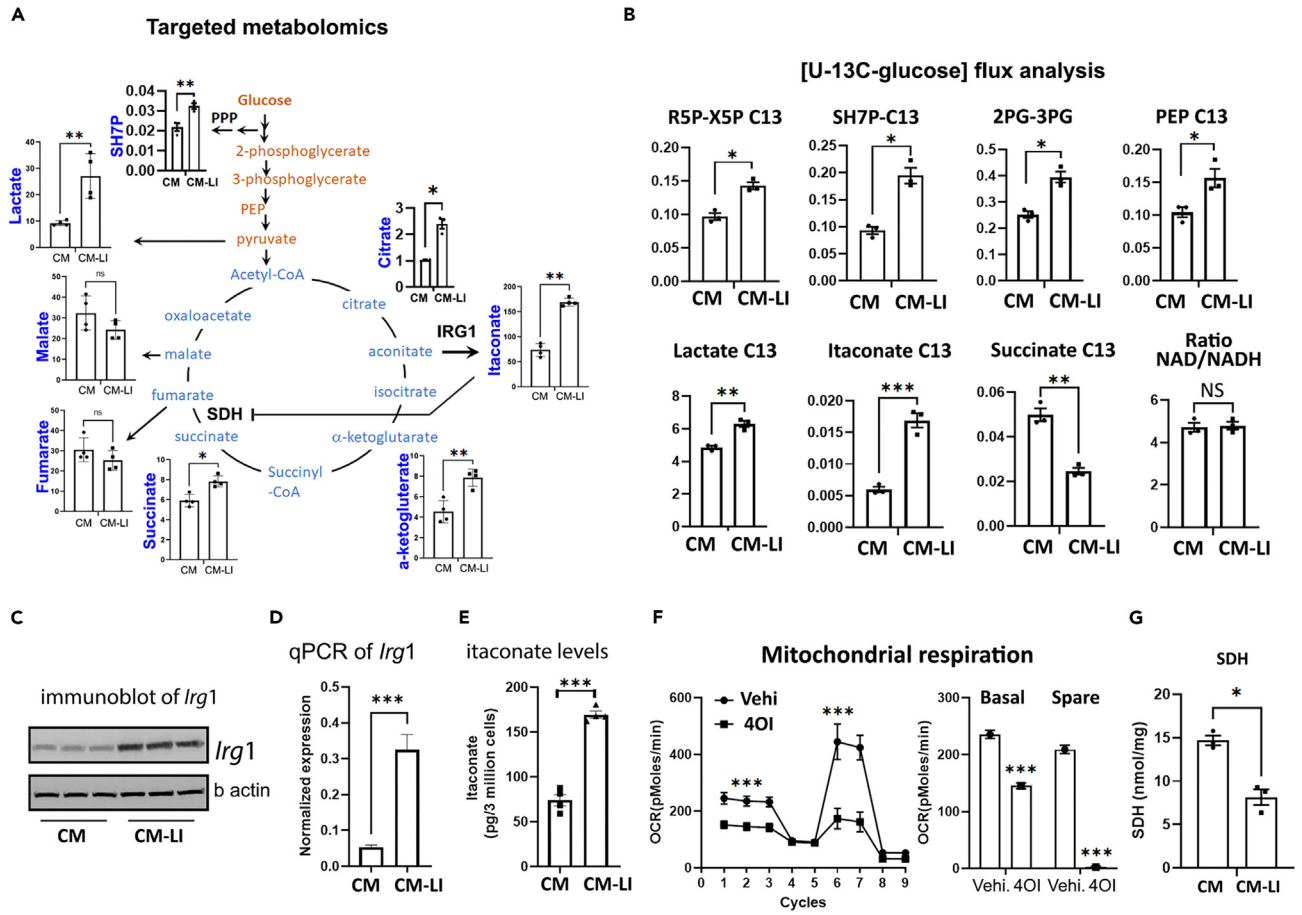

Figure 9. Itaconate is produced in CM-LI-treated oligodendrocytes and caused mitochondrial respiration failure

(A) Targeted glycolysis-TCA metabolomics was performed in CM and CM-LI treated oligodendrocytes post 18 h of treatment. Data represents two independent experiments.

(B) Incorporation of ^{13}C-carbon derived from [U-^{13}C]-Glucose into various metabolites of glycolytic and TCA cycles of CM and CM-LI treated oligodendrocytes post 8 h of treatment (N = 3).

(C and D) Expression of immune response gene 1 (*Irg1*) at protein and RNA levels by immunoblot and qPCR (N = 3).

(E) Itaconate levels in primary oligodendrocytes treated with CM or CM-LI were examined post 18 h of treatment using LC-MS/MS as under methods (N = 4).

(F) OCR in primary oligodendrocytes treated with 4-octyl itaconate (4OI, 250 μM) after 8 h of treatment. DMSO (0.1%) was used as a vehicle (N = 5). Basal and spare respiration is presented as a bar graph (N = 5).

(G) Succinate dehydrogenate (SDH) activity was measured in CM and CM-LI treated oligodendrocytes post 8 h of treatment using SDH activity assay kit (Creative BioMart) (N = 3).

For (A, B, and D–G) data are shown as mean ± SD. p values were calculated using a one-way ANOVA compared to control conditioned media (CM) groups.

oligodendrocytes could be contributed from microglia. To address this possibility, we examined the levels of itaconate in conditioned media and were unable to detect its levels in CM-LI (Figure S7Eii). Itaconate has recently been studied as a link between metabolism and immunity, and it has immunomodulatory properties.[33,34] We investigated the direct effect of cell permeable itaconate (4-octyl itaconate; 4OI) on mitochondrial respiration in oligodendrocytes because it inhibited succinate dehydrogenase[35] and rewired cellular metabolism.[33] Figure 9F shows that after 8 h of treatment, 4OI at a dose of 250 μM induced a significant reduction in mitochondrial respiration, as evidenced by a decrease in basal respiration and spare capacity compared to vehicle (0.1% DMSO) treated oligodendrocyte. Furthermore, CM-LI treated oligodendrocytes exhibited reduced activity of SDH compared to CM-treatment (Figure 9G). As previously reported,[35] the inhibition of SDH activity by 4OI treatment results in a decrease in mitochondrial respiration in oligodendrocytes. These data suggest that itaconate may play a role in oligodendrocyte mitochondrial dysfunction when treated with CM-LI from primary microglia. Itaconate production in CM-LI-treated oligodendrocytes could be partly mediated by NO, as GSNO treatment had a trending effect on itaconate production in oligodendrocytes (Figure S8). Overall, our findings shed light on the interactions between microglia and oligodendrocytes by elucidating the mechanism of metabolically controlled inflammation in primary microglia and how it affected oligodendrocyte metabolism and function via two distinct

and independent mechanisms (NO and itaconate) (Graphic abstract), influencing remyelination in neuroinflammatory and demyelinating diseases.

DISCUSSION

Our findings shed light on the mechanism of microglia-induced mitochondrial dysfunction in oligodendrocytes, which results in the loss of myelin gene expression. Neuroinflammation is emerging as a key pathological driver in many neurological diseases and neuroinflammatory processes, as well as mitochondrial dysfunction, increase the production of RNS and ROS, resulting in nitrosative stress. Stress causes metabolic reprogramming in oligodendrocytes, making them vulnerable to mature or cell death.[36,37] Microglia, the brain's resident immune cells, are the first to respond to tissue damage and initiate an inflammatory response. Activated microglia produce inflammatory cytokines and ROS/RNS, which have been shown to cause neuron and oligodendrocyte cell death. NO has been shown to cause apoptotic oligodendrocyte cell death[15,16]; however, the mechanism is unknown. The disappearance of mature, demyelinated oligodendrocytes from chronic MS lesion areas could be due to either demyelinated oligodendrocyte loss or failure of the oligodendrocyte precursor population to expand and generate new oligodendrocytes.[38–40] In chronic MS brain lesions and the demyelinated MS spinal cord, a significant number of oligodendrocyte precursor cells are present in a relatively dormant state.[39,41] Oligodendrocytes can die depending on the state of mitochondrial function.[42] Because mitochondrial respiration in demyelinated oligodendrocytes or oligodendrocyte precursor cells cannot be studied in postmortem MS brain, linking mitochondrial dysfunction in patient demyelinated oligodendrocytes or oligodendrocyte precursor cells is a limitation. Cell culture studies, on the other hand, could help define the potential mechanism of mitochondrial dysfunction in oligodendrocytes.

We found that oligodendrocytes cultured in microglial-LI-CM had mitochondrial dysfunction and expressed significantly lower levels of myelin genes than microglia-CM treated condition without affecting cell viability. A non-lethal dose of oligomycin reduced the expression of myelin proteins in oligodendrocytes, implying that mitochondrial dysfunction leads to decreased oligodendrocyte function. Despite mitochondrial dysfunction, oligodendrocytes maintained intracellular ATP levels, implying that glucose metabolism could be the source of ATP generation and survival in the absence of mitochondrial respiration. It has been reported that unlike rodent oligodendrocytes, glycolysis is the main metabolic pathway contributing in ATP production in human oligodendrocytes and oligodendrocyte precursor cells.[43] Under inflammatory condition, the metabolic demand shifted to glycolysis from mitochondrial respiration which is beneficial for limiting the production of ROS and promote lipid synthesis for myelination.[44,45] Moreover, lactate could be used as an alternative energy source in oligodendrocytes[46] and axons.[47] This cell-culture observation raised the possibility that, while pre-oligodendrocyte and oligodendrocyte precursor cells are abundant in chronic MS lesions, they are unable to differentiate into mature oligodendrocytes due to mitochondrial dysfunction. Oligodendrocyte precursor cells remain dormant and survive, possibly using glycolysis to generate energy. Conditional Cox10 (protoheme IX farnesyltransferase) mutant mice were used in a recent study, in which oligodendrocytes and Schwann cells failed to assemble stable mitochondrial cytochrome *c* oxidase (COX, also known as mitochondrial complex IV). They demonstrated that mature oligodendrocytes can survive mitochondrial dysfunction and can support axons by switching their energy demands to glycolysis in the event of an energy deficiency,[48] which is consistent what we observed *in vitro* study. Using SCENITH, we observed a metabolic derangement in microglia and oligodendrocytes in endotoxemia and preclinical mouse model of MS (EAE) suggesting that these cells undergo metabolic reprogramming under neuroinflammation, possibly playing a role in defining their effector functions. However, outcome from these *in vitro* models can't imply any crosstalk between these two cell types since other proinflammatory immune cells infiltrated in CNS especially in EAE. Therefore, we employed co-culture strategy to decipher the potential mechanism of oligodendrocyte's mitochondrial dysfunction caused by activated microglia.

Progressive MS has been linked to a decrease in complex IV and mitochondrial activity within demyelinating axons.[11] It has never been investigated whether mitochondrial dysfunction in oligodendrocytes plays a role in disease pathology. In our cell culture-based study, we found no changes in the protein expression of all five mitochondrial complex subunits in oligodendrocytes cultured in microglial-LI-CM. suggesting that mitochondrial dysfunction is caused by metabolic reprogramming rather than loss of mitochondrial proteins. Previous research[49,50] have demonstrated the importance of a metabolic switch to glycolysis during myeloid cell inflammatory responses. Glycolytic metabolism is also linked to increased lactate production, which boosts LPS-stimulated proinflammatory macrophage activation.[51] Although there is evidence of increased glucose uptake and glycolysis in activated microglial cells; in BV2[52] cells, there is no information on the role of the early glycolytic response in the production of NO by activated microglia. Increased glycolysis also sends glycolytic intermediates like 3-phosphoglycerate to the pentose phosphate pathway (PPP), which has been linked to a proinflammatory response in immune cells.[53] It is unknown whether modulating the early glycolytic response and the PPP pathway in microglia and astrocytes can affect oligodendrocyte mitochondrial function and survival. Surprisingly, only microglia exhibit an early burst of glycolysis in response to stimulation, not astrocytes (Figures S9A and S9B). Furthermore, astrocytic-LI-CM had no effect on oligodendrocyte mitochondrial respiration (Figures S9C and S9D). This could be due to the lower expression of iNOS and lesser production of NO in astrocytes compared to microglia under inflammatory condition (Figures S9E and S9F). Although we do not deny the crosstalk between astrocytes and oligodendrocytes during inflammation, under our experimental design, we believe that microglia have a more profound pathological impact on oligodendrocytes under inflammatory conditions.

We identified that PDPK1 and Akt signaling are involved in glycolytic burst in primary microglia in response to LI stimulation. TLR4-induced glycolytic burst and dendritic cell activation are dependent on AKT-mediated association of the glycolytic enzyme HKII with mitochondria.[16] AKT activation increases glycolysis by phosphorylating PFK[54] and hexokinase.[55] Inhibiting AKT signaling also prevented early

bursts of glycolysis and the production of inflammatory cytokines in primary microglia, implying a common mechanism in microglia and dendritic cell activation. We discovered that TLR4/IFN signaling can drive early metabolic changes that occur in response to microglial activation using the Seahorse bioanalyzer. An initial burst of metabolic reprogramming is required for the activation of microglia and microglia-driven factors like cytokines and NO. Although proinflammatory cytokines such as TNF and IL1β have been shown to be toxic and inhibit myelin gene expression in oligodendrocytes.[8,56] Th1-producing IFNγ-induced STAT1 signaling has been found to negatively affect oligodendrocyte[57] and its bioenergetic[58] in CNS autoimmunity. Unlike other studies that used 5– to 10-fold higher concentrations of IFNγ (100 ng/mL),[58–60] we did not notice any significant changes in the bioenergetics of oligodendrocytes when we treated with lower doses (10 ng/mL). Instead of focusing on the direct impact of cytokines on oligodendrocytes, we were more interested in examining the crosstalk between microglia and oligodendrocytes under inflammatory condition. Future research will be planned to understand how certain cytokines produced by microglia contribute to the metabolic dysfunction of oligodendrocytes under our experimental circumstances.

Our methodical series of experiments revealed that microglial driven NO causes mitochondrial failure and malfunction of oligodendrocytes. Other studies have shown that NO causes cell death,[9,61,62] which contradicts our findings. Previous research relied on NO donors, which can result in abnormally high levels of NO release at non-physiological levels.[9,61,62] We also identified that NO donors cause mitochondrial failure in oligodendrocytes after only a few hours of treatment. NO-mediated mitochondrial dysfunction in oligodendrocytes may be caused by cysteine S-nitrosylation of mitochondrial proteins involved in complex 1[29,30] as well as various enzymes involved in glycolysis, gluconeogenesis, TCA, and oxidative phosphorylation, implying that NO exposure could reprogram the metabolism of entire cells.[63] Complex 1 subunit gene therapy with NDUFA6 has been shown to improve mitochondrial dysfunction in EAE,[64] indicating the importance of complex 1 in MS pathology. In line with previous findings,[29] we discovered that NO from microglia induced nitrosylation of various proteins in oligodendrocyte. NO frequently uses guanylyl cyclase as an immediate downstream effector molecule, which catalyzes the formation of cGMP to modulate downstream functions. The NO-cGMP has been shown to have a protective effect in oligodendrocytes[65]; further research will be conducted to determine the potential role of the NO-cGMP-dependent pathway in controlling mitochondrial dysfunction in oligodendrocytes during cross-talk with microglia using *in vitro* approach. One could argue that metabolic pathways are ubiquitous, making it difficult to target them in activated microglia without affecting other cell types involved in neuroprotection and repair. We observed that in general oligodendrocytes require mitochondrial respiration, whereas activated microglia require glycolysis, however, under inflammatory condition, oligodendrocytes could survive by switching their energy source to glycolysis. More *in vivo* research is needed to confirm our cell-based findings.

Aside from NO, our untargeted metabolomics oligodendrocytes treated with CM-LI revealed itaconate as a potential endogenous immunomodulatory metabolite,[33,34] which has been shown to affect cellular metabolism. Although itaconate is also produced by microglia, it is not secreted in the media rule out the assumption that microglia derived itaconate is also involved in oligodendrocyte metabolic derangement. In fact, increased itaconate levels in oligodendrocytes under inflammatory conditions were endogenously generated from glucose metabolism, as confirmed by ^{13}C-glucose SIRM. Reduced mitochondrial respiration and levels of fumarate and malate, which are produced from succinate, a reaction catalyzed by SDH in the TCA cycle, were found to be positively linked with decreased SDH activity in CM-LI treated oligodendrocytes. Although CM-LI treatment decreased mitochondrial respiration in oligodendrocytes, it did not totally abolish because itaconate, alpha-ketoglutarate, and succinate levels increased in this experimental condition. Given that itaconate inhibits SDH activity,[35] it could be one of the mechanisms involved in the downregulation of mitochondrial function in oligodendrocytes. These findings raise the question of whether itaconate-mediated mitochondrial dysfunction is beneficial or harmful to oligodendrocytes. Because itaconate is protective in a variety of inflammatory and demyelinating diseases, one could speculate that itaconate production in cells is a protective mechanism to fight inflammatory conditions while also increasing antioxidant defense. However, more extensive research is required to establish this fact.

Overall, our findings shed a light on the communication between microglia and oligodendrocytes during inflammation. Microglial inflammatory outburst may impair the mitochondrial respiration of oligodendrocyte precursor cells/pre oligodendrocyte, thereby impeding their maturation into myelinating oligodendrocytes. Since mitochondrial respiration increases during differentiation of oligodendrocyte precursor cells into pre-oligodendrocytes,[66] our study demonstrates that microglial neuroinflammation may influence remyelination by inhibiting cellular respiration in pre oligodendrocyte. In microglia, we discovered a potential therapeutic signaling cascade: an early burst of glycolysis mediated by PDPK1 and AKT, which is responsible for increased NO and could be used as therapeutic targets to restore mitochondrial function in oligodendrocytes to promote remyelination. Itaconate was identified in oligodendrocytes as a potential endogenous metabolite in controlling mitochondrial function under inflammatory conditions, but its function in oligodendrocytes has yet to be determined.

Limitations of the study

Our *in vitro* studies clearly outlined how a signaling cascade, inflammation-PDPK1-AKT-glycolytic burst-cytokines-iNOS-NO in activated microglia could impair mitochondrial function and myelin production in oligodendrocyte, however, such mechanism cannot be replicated in an *in vivo* model at this time due to the lack of tools that can detect cell-specific early glycolytic changes and mitochondrial respiration in live animals. Despite this technological limitation, our research gives a wealth of information and a deep understanding of the interaction of two glial populations during inflammation.

STAR★METHODS

Detailed methods are provided in the online version of this paper and include the following:

- KEY RESOURCES TABLE
- RESOURCE AVAILABILITY
  - Lead contact
  - Materials availability
  - Data and code availability
- EXPERIMENTAL MODEL AND STUDY PARTICIPANT DETAILS
  - Primary brain glial culture
  - *In vivo* models
- METHOD DETAILS
  - Brain glial cell stimulation
  - Preparation of microglia-conditioned media
  - Quantitation of lipopolysaccharide (LPS) in media using UPLC-MS/MS
  - Cell viability assays
  - Nitrite concentration
  - Bioenergetic assays
  - Measurement of ATP levels in microglia and oligodendrocytes
  - Bioenergetics (OCR & ECAR) estimation in glial cells in adherent condition
  - Early glycolytic ECAR estimation in microglia
  - Assessing metabolic fitness of microglia and O4 positive oligodendrocytes *in vivo* models using single-cell energetic metabolism by profiling translation inhibition (SCENITH)
  - Western Blot analysis
  - RNA extraction, cDNA synthesis and quantitative PCR
  - Immunocytochemistry (ICC)
  - Antisense experiment
  - Targeted metabolomics
- QUANTIFICATION AND STATISTICAL ANALYSIS

SUPPLEMENTAL INFORMATION

Supplemental information can be found online at https://doi.org/10.1016/j.isci.2023.107921.

ACKNOWLEDGMENTS

This work is in-part supported by research grants from the National Multiple Sclerosis Society (US) (RG-2111-38733), the National Institutes of Health (NS112727, AI144004) and Henry Ford Hospital Internal support (A10270, A30967) to SG. The funders had no role in study design, data collection, and interpretation, or the decision to submit the work for publication.

AUTHOR CONTRIBUTIONS

H.S., M.N., F.R., M.S., M.F., J.S., I.Z., W.C., N.T., and K.A. performed experiments and finalized the manuscript, A.K., N.H., and R.R. analyzed data and finalized the manuscript, S.G. conceive the idea, directed the study, designed experiments, wrote and finalized the manuscript.

DECLARATION OF INTERESTS

The authors declare no competing interests.

INCLUSION AND DIVERSITY

We support inclusive, diverse, and equitable conduct of research.

Received: November 28, 2022
Revised: July 10, 2023
Accepted: September 12, 2023
Published: September 15, 2023

REFERENCES

1. Ferrari, C.C., Pott Godoy, M.C., Tarelli, R., Chertoff, M., Depino, A.M., and Pitossi, F.J. (2006). Progressive neurodegeneration and motor disabilities induced by chronic expression of IL-1beta in the substantia nigra. Neurobiol. Dis. *24*, 183–193. https://doi.org/10.1016/j.nbd.2006.06.013.
2. Hsiao, H.Y., Chen, Y.C., Chen, H.M., Tu, P.H., and Chern, Y. (2013). A critical role of astrocyte-mediated nuclear factor-kappaB-dependent inflammation in Huntington's disease. Hum. Mol. Genet. *22*, 1826–1842. https://doi.org/10.1093/hmg/ddt036.
3. Kassa, R.M., Mariotti, R., Bonaconsa, M., Bertini, G., and Bentivoglio, M. (2009). Gene, cell, and axon changes in the familial amyotrophic lateral sclerosis mouse sensorimotor cortex. J. Neuropathol. Exp. Neurol. *68*, 59–72. https://doi.org/10.1097/NEN.0b013e3181922572.
4. Pittock, S.J., and Lucchinetti, C.F. (2007). The pathology of MS: new insights and potential clinical applications. Neurol. *13*, 45–56. https://doi.org/10.1097/01.nrl.0000253065.31662.37.
5. Herculano-Houzel, S. (2014). The glia/neuron ratio: how it varies uniformly across brain structures and species and what that means for brain physiology and evolution. Glia *62*, 1377–1391. https://doi.org/10.1002/glia.22683.
6. Zuchero, J.B., and Barres, B.A. (2015). Glia in mammalian development and disease. Development *142*, 3805–3809. https://doi.org/10.1242/dev.129304.
7. Hellwig, S., Heinrich, A., and Biber, K. (2013). The brain's best friend: microglial neurotoxicity revisited. Front. Cell. Neurosci. *7*, 71. https://doi.org/10.3389/fncel.2013.00071.
8. Jana, M., and Pahan, K. (2005). Redox regulation of cytokine-mediated inhibition of myelin gene expression in human primary oligodendrocytes. Free Radic. Biol. Med. *39*, 823–831. https://doi.org/10.1016/j.freeradbiomed.2005.05.014.
9. Mitrovic, B., Ignarro, L.J., Vinters, H.V., Akers, M.A., Schmid, I., Uittenbogaart, C., and Merrill, J.E. (1995). Nitric oxide induces necrotic but not apoptotic cell death in oligodendrocytes. Neuroscience *65*, 531–539.
10. Dutta, R., McDonough, J., Yin, X., Peterson, J., Chang, A., Torres, T., Gudz, T., Macklin, W.B., Lewis, D.A., Fox, R.J., et al. (2006). Mitochondrial dysfunction as a cause of axonal degeneration in multiple sclerosis patients. Ann. Neurol. *59*, 478–489. https://doi.org/10.1002/ana.20736.
11. Mahad, D.J., Ziabreva, I., Campbell, G., Lax, N., White, K., Hanson, P.S., Lassmann, H., and Turnbull, D.M. (2009). Mitochondrial changes within axons in multiple sclerosis. Brain *132*, 1161–1174. https://doi.org/10.1093/brain/awp046.
12. Mahad, D., Ziabreva, I., Lassmann, H., and Turnbull, D. (2008). Mitochondrial defects in acute multiple sclerosis lesions. Brain *131*, 1722–1735. https://doi.org/10.1093/brain/awn105.
13. Nikić, I., Merkler, D., Sorbara, C., Brinkoetter, M., Kreutzfeldt, M., Bareyre, F.M., Brück, W., Bishop, D., Misgeld, T., and Kerschensteiner, M. (2011). A reversible form of axon damage in experimental autoimmune encephalomyelitis and multiple sclerosis. Nat. Med. *17*, 495–499. https://doi.org/10.1038/nm.2324.
14. Witte, M.E., Mahad, D.J., Lassmann, H., and van Horssen, J. (2014). Mitochondrial dysfunction contributes to neurodegeneration in multiple sclerosis. Trends Mol. Med. *20*, 179–187. https://doi.org/10.1016/j.molmed.2013.11.007.
15. Van den Bossche, J., Baardman, J., Otto, N.A., van der Velden, S., Neele, A.E., van den Berg, S.M., Luque-Martin, R., Chen, H.J., Boshuizen, M.C.S., Ahmed, M., et al. (2016). Mitochondrial Dysfunction Prevents Repolarization of Inflammatory Macrophages. Cell Rep. *17*, 684–696. https://doi.org/10.1016/j.celrep.2016.09.008.
16. Everts, B., Amiel, E., Huang, S.C.C., Smith, A.M., Chang, C.H., Lam, W.Y., Redmann, V., Freitas, T.C., Blagih, J., van der Windt, G.J.W., et al. (2014). TLR-driven early glycolytic reprogramming via the kinases TBK1-IKKvarepsilon supports the anabolic demands of dendritic cell activation. Nat. Immunol. *15*, 323–332. https://doi.org/10.1038/ni.2833.
17. Subhramanyam, C.S., Wang, C., Hu, Q., and Dheen, S.T. (2019). Microglia-mediated neuroinflammation in neurodegenerative diseases. Semin. Cell Dev. Biol. *94*, 112–120. https://doi.org/10.1016/j.semcdb.2019.05.004.
18. Voet, S., Prinz, M., and van Loo, G. (2019). Microglia in Central Nervous System Inflammation and Multiple Sclerosis Pathology. Trends Mol. Med. *25*, 112–123. https://doi.org/10.1016/j.molmed.2018.11.005.
19. Schubert, D., Heinemann, S., Carlisle, W., Tarikas, H., Kimes, B., Patrick, J., Steinbach, J.H., Culp, W., and Brandt, B.L. (1974). Clonal cell lines from the rat central nervous system. Nature *249*, 224–227. https://doi.org/10.1038/249224a0.
20. Roth, A.D., Leisewitz, A.V., Jung, J.E., Cassina, P., Barbeito, L., Inestrosa, N.C., and Bronfman, M. (2003). PPAR gamma activators induce growth arrest and process extension in B12 oligodendrocyte-like cells and terminal differentiation of cultured oligodendrocytes. J. Neurosci. Res. *72*, 425–435. https://doi.org/10.1002/jnr.10596.
21. Catorce, M.N., and Gevorkian, G. (2016). LPS-induced Murine Neuroinflammation Model: Main Features and Suitability for Pre-clinical Assessment of Nutraceuticals. Curr. Neuropharmacol. *14*, 155–164. https://doi.org/10.2174/1570159x14666151204122017.
22. Adamik, J., Munson, P.V., Hartmann, F.J., Combes, A.J., Pierre, P., Krummel, M.F., Bendall, S.C., Argüello, R.J., and Butterfield, L.H. (2022). Distinct metabolic states guide maturation of inflammatory and tolerogenic dendritic cells. Nat. Commun. *13*, 5184. https://doi.org/10.1038/s41467-022-32849-1.
23. Arguello, R.J., Combes, A.J., Char, R., Gigan, J.P., Baaziz, A.I., Bousiquot, E., Camosseto, V., Samad, B., Tsui, J., Yan, P., et al. (2020). SCENITH: A Flow Cytometry-Based Method to Functionally Profile Energy Metabolism with Single-Cell Resolution. Cell Metabol. *32*, 1063–1075.e1067. https://doi.org/10.1016/j.cmet.2020.11.007.
24. Lopes, N., McIntyre, C., Martin, S., Raverdeau, M., Sumaria, N., Kohlgruber, A.C., Fiala, G.J., Agudelo, L.Z., Dyck, L., Kane, H., et al. (2021). Distinct metabolic programs established in the thymus control effector functions of gammadelta T cell subsets in tumor microenvironments. Nat. Immunol. *22*, 179–192. https://doi.org/10.1038/s41590-020-00848-3.
25. Piques, M., Schulze, W.X., Höhne, M., Usadel, B., Gibon, Y., Rohwer, J., and Stitt, M. (2009). Ribosome and transcript copy numbers, polysome occupancy and enzyme dynamics in Arabidopsis. Mol. Syst. Biol. *5*, 314. https://doi.org/10.1038/msb.2009.68.
26. Alessi, D.R., James, S.R., Downes, C.P., Holmes, A.B., Gaffney, P.R., Reese, C.B., and Cohen, P. (1997). Characterization of a 3-phosphoinositide-dependent protein kinase which phosphorylates and activates protein kinase Balpha. Curr. Biol. *7*, 261–269.
27. Hannibal, L. (2016). Nitric Oxide Homeostasis in Neurodegenerative Diseases. Curr. Alzheimer Res. *13*, 135–149.
28. Saha, R.N., and Pahan, K. (2006). Regulation of inducible nitric oxide synthase gene in glial cells. Antioxidants Redox Signal. *8*, 929–947. https://doi.org/10.1089/ars.2006.8.929.
29. Clementi, E., Brown, G.C., Feelisch, M., and Moncada, S. (1998). Persistent inhibition of cell respiration by nitric oxide: crucial role of S-nitrosylation of mitochondrial complex I and protective action of glutathione. Proc. Natl. Acad. Sci. USA *95*, 7631–7636.
30. Brown, G.C., and Borutaite, V. (2004). Inhibition of mitochondrial respiratory complex I by nitric oxide, peroxynitrite and S-nitrosothiols. Biochim. Biophys. Acta *1658*, 44–49. https://doi.org/10.1016/j.bbabio.2004.03.016.
31. Michelucci, A., Cordes, T., Ghelfi, J., Pailot, A., Reiling, N., Goldmann, O., Binz, T., Wegner, A., Tallam, A., Rausell, A., et al. (2013). Immune-responsive gene 1 protein links metabolism to immunity by catalyzing itaconic acid production. Proc. Natl. Acad. Sci. USA *110*, 7820–7825. https://doi.org/10.1073/pnas.1218599110.
32. Hooftman, A., and O'Neill, L.A.J. (2019). The Immunomodulatory Potential of the Metabolite Itaconate. Trends Immunol. *40*, 687–698. https://doi.org/10.1016/j.it.2019.05.007.
33. O'Neill, L.A.J., and Artyomov, M.N. (2019). Itaconate: the poster child of metabolic reprogramming in macrophage function. Nat. Rev. Immunol. *19*, 273–281. https://doi.org/10.1038/s41577-019-0128-5.
34. Ryan, D.G., and O'Neill, L.A.J. (2020). Krebs Cycle Reborn in Macrophage Immunometabolism. Annu. Rev. Immunol. *38*, 289–313. https://doi.org/10.1146/annurev-immunol-081619-104850.
35. Lampropoulou, V., Sergushichev, A., Bambouskova, M., Nair, S., Vincent, E.E., Loginicheva, E., Cervantes-Barragan, L., Ma, X., Huang, S.C.C., Griss, T., et al. (2016). Itaconate Links Inhibition of Succinate Dehydrogenase with Macrophage Metabolic Remodeling and Regulation of Inflammation. Cell Metabol. *24*, 158–166. https://doi.org/10.1016/j.cmet.2016.06.004.
36. French, H.M., Reid, M., Mamontov, P., Simmons, R.A., and Grinspan, J.B. (2009). Oxidative stress disrupts oligodendrocyte maturation. J. Neurosci. Res. *87*, 3076–3087. https://doi.org/10.1002/jnr.22139.
37. Spaas, J., van Veggel, L., Schepers, M., Tiane, A., van Horssen, J., Wilson, D.M., 3rd, Moya, P.R., Piccart, E., Hellings, N., Eijnde, B.O., et al. (2021). Oxidative stress and impaired oligodendrocyte precursor cell

differentiation in neurological disorders. Cell. Mol. Life Sci. *78*, 4615–4637. https://doi.org/10.1007/s00018-021-03802-0.
38. Wolswijk, G. (1998). Oligodendrocyte regeneration in the adult rodent CNS and the failure of this process in multiple sclerosis. Prog. Brain Res. *117*, 233–247. https://doi.org/10.1016/s0079-6123(08)64019-4.
39. Wolswijk, G. (1998). Chronic stage multiple sclerosis lesions contain a relatively quiescent population of oligodendrocyte precursor cells. J. Neurosci. *18*, 601–609. https://doi.org/10.1523/JNEUROSCI.18-02-00601.1998.
40. Wolswijk, G. (2000). Oligodendrocyte survival, loss and birth in lesions of chronic-stage multiple sclerosis. Brain *123*, 105–115. https://doi.org/10.1093/brain/123.1.105.
41. Wolswijk, G. (2002). Oligodendrocyte precursor cells in the demyelinated multiple sclerosis spinal cord. Brain *125*, 338–349. https://doi.org/10.1093/brain/awf031.
42. Casaccia-Bonnefil, P. (2000). Cell death in the oligodendrocyte lineage: a molecular perspective of life/death decisions in development and disease. Glia *29*, 124–135.
43. Rone, M.B., Cui, Q.L., Fang, J., Wang, L.C., Zhang, J., Khan, D., Bedard, M., Almazan, G., Ludwin, S.K., Jones, R., et al. (2016). Oligodendrogliopathy in Multiple Sclerosis: Low Glycolytic Metabolic Rate Promotes Oligodendrocyte Survival. J. Neurosci. *36*, 4698–4707. https://doi.org/10.1523/JNEUROSCI.4077-15.2016.
44. Brand, K.A., and Hermfisse, U. (1997). Aerobic glycolysis by proliferating cells: a protective strategy against reactive oxygen species. Faseb. J. *11*, 388–395. https://doi.org/10.1096/fasebj.11.5.9141507.
45. Bongarzone, E.R., Pasquini, J.M., and Soto, E.F. (1995). Oxidative damage to proteins and lipids of CNS myelin produced by in vitro generated reactive oxygen species. J. Neurosci. Res. *41*, 213–221. https://doi.org/10.1002/jnr.490410209.
46. Sánchez-Abarca, L.I., Tabernero, A., and Medina, J.M. (2001). Oligodendrocytes use lactate as a source of energy and as a precursor of lipids. Glia *36*, 321–329.
47. Lee, Y., Morrison, B.M., Li, Y., Lengacher, S., Farah, M.H., Hoffman, P.N., Liu, Y., Tsingalia, A., Jin, L., Zhang, P.W., et al. (2012). Oligodendroglia metabolically support axons and contribute to neurodegeneration. Nature *487*, 443–448. https://doi.org/10.1038/nature11314.
48. Fünfschilling, U., Supplie, L.M., Mahad, D., Boretius, S., Saab, A.S., Edgar, J., Brinkmann, B.G., Kassmann, C.M., Tzvetanova, I.D., Möbius, W., et al. (2012). Glycolytic oligodendrocytes maintain myelin and long-term axonal integrity. Nature *485*, 517–521. https://doi.org/10.1038/nature11007.
49. Soto-Heredero, G., Gómez de Las Heras, M.M., Gabandé-Rodríguez, E., Oller, J., and Mittelbrunn, M. (2020). Glycolysis - a key player in the inflammatory response. FEBS J. *287*, 3350–3369. https://doi.org/10.1111/febs.15327.
50. Kelly, B., and O'Neill, L.A.J. (2015). Metabolic reprogramming in macrophages and dendritic cells in innate immunity. Cell Res. *25*, 771–784. https://doi.org/10.1038/cr.2015.68.
51. Nareika, A., He, L., Game, B.A., Slate, E.H., Sanders, J.J., London, S.D., Lopes-Virella, M.F., and Huang, Y. (2005). Sodium lactate increases LPS-stimulated MMP and cytokine expression in U937 histiocytes by enhancing AP-1 and NF-kappaB transcriptional activities. Am. J. Physiol. Endocrinol. Metab. *289*, E534–E542. https://doi.org/10.1152/ajpendo.00462.2004.
52. Gimeno-Bayón, J., López-López, A., Rodríguez, M.J., and Mahy, N. (2014). Glucose pathways adaptation supports acquisition of activated microglia phenotype. J. Neurosci. Res. *92*, 723–731. https://doi.org/10.1002/jnr.23356.
53. Perl, A., Hanczko, R., Telarico, T., Oaks, Z., and Landas, S. (2011). Oxidative stress, inflammation and carcinogenesis are controlled through the pentose phosphate pathway by transaldolase. Trends Mol. Med. *17*, 395–403. https://doi.org/10.1016/j.molmed.2011.01.014.
54. Novellasdemunt, L., Tato, I., Navarro-Sabate, A., Ruiz-Meana, M., Méndez-Lucas, A., Perales, J.C., Garcia-Dorado, D., Ventura, F., Bartrons, R., and Rosa, J.L. (2013). Akt-dependent activation of the heart 6-phosphofructo-2-kinase/fructose-2,6-bisphosphatase (PFKFB2) isoenzyme by amino acids. J. Biol. Chem. *288*, 10640–10651. https://doi.org/10.1074/jbc.M113.455998.
55. Roberts, D.J., Tan-Sah, V.P., Smith, J.M., and Miyamoto, S. (2013). Akt phosphorylates HK-II at Thr-473 and increases mitochondrial HK-II association to protect cardiomyocytes. J. Biol. Chem. *288*, 23798–23806. https://doi.org/10.1074/jbc.M113.482026.
56. Li, J., Ramenaden, E.R., Peng, J., Koito, H., Volpe, J.J., and Rosenberg, P.A. (2008). Tumor necrosis factor alpha mediates lipopolysaccharide-induced microglial toxicity to developing oligodendrocytes when astrocytes are present. J. Neurosci. *28*, 5321–5330. https://doi.org/10.1523/JNEUROSCI.3995-07.2008.
57. Lin, W., and Lin, Y. (2010). Interferon-gamma inhibits central nervous system myelination through both STAT1-dependent and STAT1-independent pathways. J. Neurosci. Res. *88*, 2569–2577. https://doi.org/10.1002/jnr.22425.
58. Minchenberg, S.B., and Massa, P.T. (2019). The control of oligodendrocyte bioenergetics by interferon-gamma (IFN-gamma) and Src homology region 2 domain-containing phosphatase-1 (SHP-1). J. Neuroimmunol. *331*, 46–57. https://doi.org/10.1016/j.jneuroim.2017.10.015.
59. Pouly, S., Becher, B., Blain, M., and Antel, J.P. (2000). Interferon-gamma modulates human oligodendrocyte susceptibility to Fas-mediated apoptosis. J. Neuropathol. Exp. Neurol. *59*, 280–286. https://doi.org/10.1093/jnen/59.4.280.
60. Tirotta, E., Ransohoff, R.M., and Lane, T.E. (2011). CXCR2 signaling protects oligodendrocyte progenitor cells from IFN-gamma/CXCL10-mediated apoptosis. Glia *59*, 1518–1528. https://doi.org/10.1002/glia.21195.
61. Baud, O., Li, J., Zhang, Y., Neve, R.L., Volpe, J.J., and Rosenberg, P.A. (2004). Nitric oxide-induced cell death in developing oligodendrocytes is associated with mitochondrial dysfunction and apoptosis-inducing factor translocation. Eur. J. Neurosci. *20*, 1713–1726. https://doi.org/10.1111/j.1460-9568.2004.03616.x.
62. Boullerne, A.I., Nedelkoska, L., and Benjamins, J.A. (1999). Synergism of nitric oxide and iron in killing the transformed murine oligodendrocyte cell line N20.1. J. Neurochem. *72*, 1050–1060.
63. Doulias, P.T., Tenopoulou, M., Greene, J.L., Raju, K., and Ischiropoulos, H. (2013). Nitric oxide regulates mitochondrial fatty acid metabolism through reversible protein S-nitrosylation. Sci. Signal. *6*, rs1. https://doi.org/10.1126/scisignal.2003252.
64. Talla, V., Koilkonda, R., Porciatti, V., Chiodo, V., Boye, S.L., Hauswirth, W.W., and Guy, J. (2015). Complex I subunit gene therapy with NDUFA6 ameliorates neurodegeneration in EAE. Invest. Ophthalmol. Vis. Sci. *56*, 1129–1140. https://doi.org/10.1167/iovs.14-15950.
65. Garthwaite, G., Hampden-Smith, K., Wilson, G.W., Goodwin, D.A., and Garthwaite, J. (2015). Nitric oxide targets oligodendrocytes and promotes their morphological differentiation. Glia *63*, 383–399. https://doi.org/10.1002/glia.22759.
66. Neumann, B., Baror, R., Zhao, C., Segel, M., Dietmann, S., Rawji, K.S., Foerster, S., McClain, C.R., Chalut, K., van Wijngaarden, P., and Franklin, R.J.M. (2019). Metformin Restores CNS Remyelination Capacity by Rejuvenating Aged Stem Cells. Cell Stem Cell *25*, 473–485.e8. https://doi.org/10.1016/j.stem.2019.08.015.
67. Giri, S., Khan, M., Nath, N., Singh, I., and Singh, A.K. (2008). The role of AMPK in psychosine mediated effects on oligodendrocytes and astrocytes: implication for Krabbe disease. J. Neurochem. *105*, 1820–1833. https://doi.org/10.1111/j.1471-4159.2008.05279.x.
68. Giri, S., Khan, M., Rattan, R., Singh, I., and Singh, A.K. (2006). Krabbe disease: psychosine-mediated activation of phospholipase A2 in oligodendrocyte cell death. J. Lipid Res. *47*, 1478–1492. https://doi.org/10.1194/jlr.M600084-JLR200.
69. Giri, S., Nath, N., Smith, B., Viollet, B., Singh, A.K., and Singh, I. (2004). 5-aminoimidazole-4-carboxamide-1-beta-4-ribofuranoside inhibits proinflammatory response in glial cells: a possible role of AMP-activated protein kinase. J. Neurosci. *24*, 479–487. https://doi.org/10.1523/JNEUROSCI.4288-03.2004.
70. Giri, S., Rattan, R., Singh, A.K., and Singh, I. (2004). The 15-deoxy-delta12,14-prostaglandin J2 inhibits the inflammatory response in primary rat astrocytes via down-regulating multiple steps in phosphatidylinositol 3-kinase-Akt-NF-kappaB-p300 pathway independent of peroxisome proliferator-activated receptor gamma. J. Immunol. *173*, 5196–5208. https://doi.org/10.4049/jimmunol.173.8.5196.
71. Zahoor, I., Suhail, H., Datta, I., Ahmed, M.E., Poisson, L.M., Waters, J., Rashid, F., Bin, R., Singh, J., Cerghet, M., et al. (2022). Blood-based untargeted metabolomics in relapsing-remitting multiple sclerosis revealed the testable therapeutic target. Proc. Natl. Acad. Sci. USA *119*, e2123265119. https://doi.org/10.1073/pnas.2123265119.
72. Hanisch, U.K., and Kettenmann, H. (2007). Microglia: active sensor and versatile effector cells in the normal and pathologic brain. Nat. Neurosci. *10*, 1387–1394. https://doi.org/10.1038/nn1997.
73. Ransohoff, R.M., and Perry, V.H. (2009). Microglial physiology: unique stimuli, specialized responses. Annu. Rev. Immunol. *27*, 119–145. https://doi.org/10.1146/annurev.immunol.021908.132528.
74. Lehnardt, S., Massillon, L., Follett, P., Jensen, F.E., Ratan, R., Rosenberg, P.A., Volpe, J.J., and Vartanian, T. (2003). Activation of innate immunity in the CNS triggers neurodegeneration through a Toll-like receptor 4-dependent pathway. Proc. Natl.

Acad. Sci. USA *100*, 8514–8519. https://doi.org/10.1073/pnas.1432609100.

75. Lee, J.Y., and Sullivan, K.E. (2001). Gamma interferon and lipopolysaccharide interact at the level of transcription to induce tumor necrosis factor alpha expression. Infect. Immun. *69*, 2847–2852. https://doi.org/10.1128/IAI.69.5.2847-2852.2001.
76. Häusler, K.G., Prinz, M., Nolte, C., Weber, J.R., Schumann, R.R., Kettenmann, H., and Hanisch, U.K. (2002). Interferon-gamma differentially modulates the release of cytokines and chemokines in lipopolysaccharide- and pneumococcal cell wall-stimulated mouse microglia and macrophages. Eur. J. Neurosci. *16*, 2113–2122. https://doi.org/10.1046/j.1460-9568.2002.02287.x.
77. Dawson, V.L., Brahmbhatt, H.P., Mong, J.A., and Dawson, T.M. (1994). Expression of inducible nitric oxide synthase causes delayed neurotoxicity in primary mixed neuronal-glial cortical cultures. Neuropharmacology *33*, 1425–1430. https://doi.org/10.1016/0028-3908(94)90045-0.
78. Pais de Barros, J.P., Gautier, T., Sali, W., Adrie, C., Choubley, H., Charron, E., Lalande, C., Le Guern, N., Deckert, V., Monchi, M., et al. (2015). Quantitative lipopolysaccharide analysis using HPLC/MS/MS and its combination with the limulus amebocyte lysate assay. J. Lipid Res. *56*, 1363–1369. https://doi.org/10.1194/jlr.D059725.
79. Dar, S., Chhina, J., Mert, I., Chitale, D., Buekers, T., Kaur, H., Giri, S., Munkarah, A., and Rattan, R. (2017). Bioenergetic Adaptations in Chemoresistant Ovarian Cancer Cells. Sci. Rep. *7*, 8760. https://doi.org/10.1038/s41598-017-09206-0.
80. Udumula, M.P., Sakr, S., Dar, S., Alvero, A.B., Ali-Fehmi, R., Abdulfatah, E., Li, J., Jiang, J., Tang, A., Buekers, T., et al. (2021). Ovarian cancer modulates the immunosuppressive function of CD11b(+) Gr1(+) myeloid cells via glutamine metabolism. Mol. Metabol. *53*, 101272. https://doi.org/10.1016/j.molmet.2021.101272.
81. Bao, X., Wu, J., Kim, S., LoRusso, P., and Li, J. (2019). Pharmacometabolomics Reveals Irinotecan Mechanism of Action in Cancer Patients. J. Clin. Pharmacol. *59*, 20–34. https://doi.org/10.1002/jcph.1275.

STAR★METHODS

KEY RESOURCES TABLE

REAGENT or RESOURCE	SOURCE	IDENTIFIER
Antibodies		
Rabbit anti-phospho-PDPK1	Cell Signaling Technology	Cat # 3438, RRID:AB_2161134
Rabbit anti-total-PDPK1	Cell Signaling Technology	Cat # 13037, RRID:AB_2798095
Rabbit anti-phospho-AKT	Cell Signaling Technology	Cat # 4060, RRID:AB_2315049
Rabbit anti-total-AKT	Cell Signaling Technology	Cat # 4691S, RRID:AB_915783
Purified Mouse Anti-Mouse iNOS	BD Bioscience	Cat # 610432, RRID:AB_397808
β-actin Monoclonal Antibody	Invitrogen	Cat # MA1-1402, RRID:AB_2536844
Goat anti-rabbit IgG (HRP conjugate)	Invitrogen	Cat # 31460, RRID:AB_228341
Goat anti-mouse IgG (HRP conjugate)	Invitrogen	Cat v# 31430, RRID:AB_228307
Rabbit anti-PLP antibody	Abcam	Cat # ab28486, RRID:AB_776593
Rabbit anti-Myelin Basic Protein antibody	Abcam	Cat # ab7349, RRID:AB_305869
Goat Anti-Rabbit IgG H&L (Cy3)	Abcam	Cat # ab6939, RRID:AB_955021
Goat Anti-Rabbit IgG (Alexa Fluor® 488)	Abcam	Cat # ab150077, RRID:AB_2630356
Anti-CD16/32	Biolegend	Cat # 101302, RRID:AB_312801
AF647-puromycin	Biolegend	Cat # 381508
BV421-CD45	Biolegend	Cat # 103134, RRID:AB_2562559
BV510-CD11b	Biolegend	#101263, RRID:AB_2629529
PerCP/Cy5.5-CD45	Biolegend	#103132, RRID:AB_893340
PE-Cy7-CD11b	Biolegend	# 101216, RRID:AB_312799
FITC-CD11b	Biolegend	# 101205, RRID:AB_312788
PE-mouse IgG, k isotype control	Biolegend	# 400212, RRID:AB_326460
BV510-Ly6G	Biolegend	# 127633, RRID:AB_2562937
PE-O4	Miltenyi Biotech	# 130-117-357, RRID:AB_2733887
Chemicals, peptides, and recombinant proteins		
Oligomycin	Cayman Chemical	Cat # 11342
FCCP	Cayman Chemical	Cat # 15218
Antimycin-A	Cayman Chemical	Cat # 19433
Rotenone	Cayman Chemical	Cat # 13995
2-Deoxyglucose (2DG)	Cayman Chemical	Cat # 17149
L-NAME (hydrochloride)	Cayman Chemical	Cat # 80210
SIN-1 (chloride)	Cayman Chemical	Cat # 82220
(R)-3-hydroxy Tetradecanoic Acid	Cayman Chemical	Cat # 16871
BX 795 (PDPK1 inhibitor)	Tocris	Cat # 4318
API-1 (Akt inhibitor)	Tocris	Cat # 3897
iNOS shRNA (m) lentiviral particles	Santa Cruz Biotech	Cat # #sc-36092-V
Control shRNA (m) lentiviral particles	Santa Cruz Biotech	Cat # sc-108080
Lipopolysaccharide	Invivogen	Cat # tlrl-eblps
Recombinant interferon gamma	Biolegend	Cat # 575306
Puromycin	Invivogen	Cat # ant-pr-1
Fetal Bovine Serum, US origin	BioAbChem	Cat # 72-0400
DMEM high glucose	Thermofisher	Cat # 11965092

(*Continued on next page*)

Continued

REAGENT or RESOURCE	SOURCE	IDENTIFIER
DMEM/F12	Thermofisher	Cat # A4192001
RPMI 1640 media without glucose	Thermofisher	Cat # 11879020
LIVE/DEAD™ Fixable Yellow Stain	Thermofisher	Cat #L34967
TCA Isotope-Labeled standard Mix 1	Cambridge isotopes	Cat # MSK-TCA1-1
TCA Isotope-Labeled standard Mix 2	Cambridge isotopes	Cat # MSK-TCA1-2
MS grade acetonitrile	Sigma Aldrich	Cat # 1000294000
MS grade Water	Sigma Aldrich	Cat # 900682
MS grade Methanol	Sigma Aldrich	Cat # 1060354000
n-Hexane	Sigma Aldrich	Cat # 1037011000
MS grade ammonium acetate	Sigma Aldrich	Cat # 5330040050
Ammonium hydroxide (10–35%)	Sigma Aldrich	Cat # 221228
Formic Acid	Sigma Aldrich	Cat # 00940
D-Glucose-$^{13}C_6$	Sigma	Cat # 389374
Triiodothyronine	Sigma	Cat #T2877
Non-fat dry milk	BioRad	Cat # 1706406XTU
MOG_{35-55} ^{peptide} (MEVGWYRSPFSRVVHLYRNGK)	GeneTex, Inc.	N/A
Critical commercial assays		
ATP detection kit	Invitrogen	Cat # A22066
Lactate assay kit	Eton Bio, Inc.	Cat # 1200011002
Glucose detection kit	Invitrogen	Cat # EIAGLUC
Seahorse FluxPak XFe96/Pro	Agilent	Cat # 103792-100
TRIzol	Thermofisher	Cat # 15596018
iScript Reverse Transcription Supermix	Bio-Rad	Cat # 1708841
iTaq Univer SYBR Green Supermix	Bio-Rad	Cat # 1725125
Softwares		
GraphPad Prism	GraphPad Software Inc.	Graph Pad Prism 9
CFX Maestro	Bio-Rad	Cat # 12013758
FlowJo	flowJo, LLC	FlowJo V10
MassLynx MS software	Waters	Mass Lynx v4.2
Experimental models: Cell lines		
Human MO3.13 oligodendroglial cells	Laboratory of Dr. Waters	Accession: CVCL_D357
Rat B12 oligodendrocyte-like cells	Laboratory of Dr. Schubert	Accession: CVCL_4111
Experimental models: Organisms/strains		
Rat: Pregnant ED15	Charles River Labs	Cat # CD (SD)
Mouse: C57/B6	The Jackson Laboratory	JAX: 000664; RRID:IMSR_JAX:000664
Oligonucleotides		
siRNA Smart pool mouse Akt1	Dharmacon	Cat # L-040709-00
siRNA Smart pool mouse PDPK1	Dharmacon	Cat # L-040658-00
Rat iNOS	Integrated DNA technology (ITD)	Fw: GGAAGAGGAACAACTACTGCTGGT Rv: GAACTGAGGGTACATGCTGGAGC
Rat IL1b	Integrated DNA technology (ITD)	Fw: CCAGGATGAGGACCCAAGCA Rv: TCCCGACCATTGCTGTTTCC
Rat IL6	Integrated DNA technology (ITD)	Fw: CTTCCAGCCAGTTGCCTTCT Rv: GACAGCATTGGAAGTTGGGG

(*Continued on next page*)

Continued

REAGENT or RESOURCE	SOURCE	IDENTIFIER
Rat TNFa	Integrated DNA technology (ITD)	Fw: CGAGTGACAAGCCCGTAGCC Rv: GGATGAACACGCCAGTCGCC
Rat MIP2	Integrated DNA technology (ITD)	Fw: CTGGTCCTGCTCCTCCTGCT Rv: TTTGATTCTGCCCGTTGAGG
Rat Glut1	Integrated DNA technology (ITD)	Fw: TGCAGTTCGGCTATAACACC Rv: ACACCTCCCCCACATACATG
rHK2	Integrated DNA technology (ITD)	Fw: TCTGCCAGATTGTGTCCACG Rv: AGTCGAAGTCTCTGAGGTCC
Rat LDHa	Integrated DNA technology (ITD)	Fw: CCGTTACCTGATGGGAGAAA Rv: ACGTTCACACCACTCCACAC
Rat MCT4	Integrated DNA technology (ITD)	Fw: TCACGGGTTTCTCCTACGC Rv: GCCAAAGCGGTTCACACAC
Rat TPI	Integrated DNA technology (ITD)	Fw: CCAGGAAGTTCTTCGTTGGGC Rv:CAAAGTCGATGTAAGCGGTGG
Rat MBP	Integrated DNA technology (ITD)	Fw: CTCTGGCAAGGACTCACACAC Rv: TCTGCTGAGGGACAGGCCTCTC
Rat MAG	Integrated DNA technology (ITD)	Fw: TGCCATCCTGATTGCCATTG Rv: CTCATACTTATCAGGTGCTCC
Rat PLP	Integrated DNA technology (ITD)	Fw: GCCTTCCCTAGCAAGACCTCTGAG Rv: GAACTTGGTGCCTCGGCCCATGAG
Rat MOG	Integrated DNA technology (ITD)	Fw: CAGAGACCACTCCTACCAAG Rv: TTCTGCACGGAGTTTTCCTCT
Rat *Irg*1	BioRad	#10041596
Rat L-27	RealTimePrimers.com	#VRPS-5294

RESOURCE AVAILABILITY

Lead contact

Further information and requests for resources and reagents should be directed to and will be fulfilled by lead contact, Shailendra Giri (sgiri1@hfhs.org).

Materials availability

This study did not generate any unique reagents.

Data and code availability

- All the data are available in the main test or the supplementary materials.
- This paper does not report original code.
- Any additional information required to reanalyze the data reported in this paper is available from the lead contact upon request.

EXPERIMENTAL MODEL AND STUDY PARTICIPANT DETAILS

Primary brain glial culture

The timed pregnant rat was purchased from Charles River Laboratory. The brains of 2-3-day old rat female and male pups were used to prepare mixed glial cell cultures. We followed our previously published protocol to prepare the primary mixed glial cell culture.[67–70] In summary, the brain was aseptically excised, and cortical cells were separated from blood vessels and meninges. The cerebral cortical cell was mechanically triturated into a single cell suspension with a Pasteur pipet and resuspended in complete media (DMEM 4.5 g/L) supplemented with 10% FBS and 10 mg/mL antibiotics. The suspended cells were seeded in 75 cm2 poly-D-lysine-coated flasks and incubated at 37°C in a humidified 5% CO2 incubator. After 24 h, the media was replaced with fresh complete DMEM (4.5 g/L) media, which was then exchanged twice a week. The cells were grown for at least 12–14 days until they reached full confluence and were ready to dissociate. The primary mixed glial culture was shaken on an orbital shaker at 37°C for 2 h at 180 rpm to obtain rat microglial cells. The floating cell media was collected into a 50 mL tube, and the flask was replenished with fresh complete DMEM (4.5 g/L) media. The floating cells collected after shaking contained 90% microglia.

For the experiment, microglia were plated in a 100 mm Petri dish. The flasks were shaken again the next day at 200 rpm for 14-16 h to obtain the primary oligodendrocytes. Cells were plated in DMEM/F12 with 0.5%FBS. Post two days, more than 92% cells expressed the oligodendroglial lineage marker O4 cells examined by flow cytometry and immunostaining (Figure S10) and used for downstream experiments.[67,68]

In vivo models

The C57B6 female mice were purchased from the Jackson Laboratories (Bar Harbor, ME) and was maintained in the pathogen-free animal housing facility at the Henry Ford Health System, Detroit, MI. All animals were housed on a standard 12 h light/12 h dark cycle with *ad libitum* access to food and water. To examine the metabolic derangement in microglia and O4+ oligodendrocytes, we used two *in vivo* models; 1) In endotoxemia, C57B6 female mice were injected with LPS (1 mg/kg body weight) in the volume of 200 μL in PBS for 6hs before harvesting brain. 2) Experimental autoimmune encephalomyelitis (EAE), an animal model of MS was used. EAE was induced in C57B6 female mice by immunizing MOG_{35-55} in CFA.[71] Control group was injected with CFA alone. Post 18 days of immunization, brain, and spinal cord of EAE and CFA groups were harvested for downstream analysis. Although we use female mice for both *in vivo* models, endotoxemia and EAE disease induction have been documented in both male and female C57B6 mice; thus, the influence of sex on the result of the *in vivo* study is not anticipated.

All experiments using animals were approved by the Henry Ford hospital Institutional Animal Care and Use Committee, an Association for Assessment and Accreditation of Laboratory Animal Care International-approved committee. The adult pregnant female rat and female C57B6 mice were maintained in the pathogen-free animal housing facility at the Henry Ford Health System, Detroit, MI.

METHOD DETAILS

Brain glial cell stimulation

After 24 h of plating, the cells were treated for the indicated time with LPS (0.5 μg/mL) + IFNγ (10 ng/mL). 1 h before LPS/IFNγ (LI) stimulation, cultures were pretreated with various inhibitors at the indicated concentrations. Combination of LPS and IFNγ are known stimuli to create *in vitro* inflammatory condition. LPS via its receptor, Toll-Like Receptor 4 (TLR4) has been widely used to study the molecular mechanisms of microglial activation in inflammatory neurodegeneration.[72,73] Moreover, Th1-deriven IFNγ signaling acts as "booster" to trigger the LPS-induced production of proinflammatory and cytotoxic factors, such as TNF-α, IL-6, and nitric oxide (NO),[74–77] therefore, we used combination of LPS/IFNγ (LI) to induce inflammatory condition for our study.

Preparation of microglia-conditioned media

In 100 mm Petri dishes, isolated microglia were plated. Next day, cells were cultured in serum-free DMEM media for 2 h prior stimulation with LPS (0.5 μg/ml) + IFNγ (10 ng/ml). Post 6 h of stimulation, petri plates were washed three times with warm serum-free DMEM media and replenished with the same media and respective inhibitors. The supernatant media was collected after 18 h and stored at −20°C for use as conditioned media (CM-LI). CM-LI did not have any contamination of LPS, detected by LC-MS/MS (Figure S3A). Conditioned media from untreated cells was used a control (CM).

Quantitation of lipopolysaccharide (LPS) in media using UPLC-MS/MS

Quantitation of LPS was performed from LPS-derived (R)-3-hydroxyl Myristate Acid (or 3-HM) extracted upon hydrolysis with hydrochloric acid. Quantitation of 3-HM from culture media (LPSs spiked-in) was performed.[78] Cell supernatant media was collected at different time interval 0 h, 6 h after addition of LPS (0.5 μg/mL). Post 6 h, cells were rinsed and washed with serum free DMEM media and further cultured cells in serum free media for additional 18 h. Media was also collected after washing at 6 h and 18 h post culture in serum free media. Briefly, 50 μL of media spiked with 125 ng of internal standard (3-HM,10 mg/mL in DMSO) was hydrolyzed with 75 μL of NaCl 150 mM and 300 μL of 8M-HCl for 4 h at 90°C. Free fatty acids were than extracted with 600 μL of distilled water and 5 mL of hexane. After vacuum evaporation of the hexane phase, fatty acids were dissolved in 100 μL 40% A/60% B eluent mixture. The upper phase (∼90 μL) containing the extracted matrix was transferred into fresh tubes, vortexed (15 min) and centrifuge for 5 min at 15,000 and placed in an UPLC vial for LC-MS/MS analysis. Waters UPLC-TQD was employed for method development including method optimization, ionization, and fragmentation. Mobile phase A (10 mM Ammonium acetate 10 mM pH 5.0) and mobile phase B (Acetonitrile/ammonium acetate 10 mM pH 7.3 (97:3)) at a flow rate of 0.5 mL/min in gradient mode. Best separation of 3-HM was achieved using RP Phenomenex Synergi Column, 130 Å, 4 μm, 2 mm × 50 mm column at 55°C. The sampler was maintained at 4°C and injected 10 μL with total running time of 6 min. TQD-MS was operated at ESI-NEG using multiple reaction monitoring (MRM) mode. TQD mass spectrometry equipped with an ESI probe: Capillary: voltage, 3.75 kV for negative mode: Source temp: 120°C: Desolvation temp: 450°C; Cone gas flow: 120 L/Hr: Desolvation gas flow:800 L/Hr Collision gas flow: 0.25 mL/min and Nebulizer gas flow: 7 Bar. For 3-HM quantification, peak area ratios (PARs) of the analyte peak area to the ISTD peak were calculated. The calibration curve, prepared in matrix, was constructed using PARs of the calibration samples by applying a one/concentration weighting (1/x) linear regression model. All quality control sample concentrations were then calculated from their PARs against the calibration curve. For limit of detection (LOD) and lower limit of quantification (LLOQ), eight calibration standards ranging from 8 to 1000 ng/mL were subjected to the full extraction procedure three times before analysis. The limit of detection (LOD) was defined as the 3-HM concentration corresponding to the lowest calibration point, where signal to noise ratio (s/n) was three times greater than from the blank signal and lower limit of quantification was signal 10 times more compared to s/n with blank. Data analysis for mass spectrometric data was acquired by MassLynx v4.2software. Enabled with

quantification software, TargetLynx software was used for preparing the calibration curve and absolute quantitation of 3-HM in the samples. The quantitative performance using this sample preparation and LC-MS method was excellent, achieving an LLOQ of 8 ng/mL for 3-HM. Calibration curves were linear (r2 > 0.997) from 8 to 1000 ng/mL.

Cell viability assays

The cellular viability was determined by measuring the cells' metabolic activity using MTT and LDH assays. The MTT and LDH release (Roche) were carried out in accordance with the established protocol. The optical density at 550 nm of a microplate reader (Bio-Rad) was used to estimate the reduction of MTT to formazan within cells (Data not shown).

Nitrite concentration

The NO released by activated microglia was measured in culture supernatants using the standard Griess reagent method.[69,70] In brief, 100 μL of culture supernatants were mixed with an equal volume of Griess reagent in 96 well plates and measured at 570 nm using a Bio-Rad microplate reader. A standard curve derived from the reaction of NaNO2 in the assay was used to estimate the Nitrite concentration.

Bioenergetic assays

The cells were grown in 6 well plate with concentration of $50x10^4$ cells/well in DMEM (10% FBS) media. After the cells reached 80–90% confluence, the indicated treatments were performed. The inhibitors were pre-treated for 1h before the LPS/IFNγ treatment. After 24 h the cells were washed with serum-free DMEM media and treated with or without 100 ng/mL oligomycin for 6 h. The supernatant media was collected and analyzed for the lactate (as per protocol by Eton Bioscience) and glucose concentration (Invitrogen Life technology) at 560 nm. For the bioenergetics assays (glycolysis vs. OXPHOS), we used the following protocols: $Lac_{(c)}$ = lactate concentration in the control medium after 6 h incubation; Glycolysis % = $Lac_{(control)} \times 100/Lac_{(oligomycin)}$; and OXPHOS % = 100 − Glycolysis %.[79]

Measurement of ATP levels in microglia and oligodendrocytes

The cells were grown in 96 well plate (25×10^4/well), and level of ATP was determined with fluorometric ATP determination kit following the manufacturer's protocol (Invitrogen). Data presented as unit/number of cells.

Bioenergetics (OCR & ECAR) estimation in glial cells in adherent condition

Seahorse Bioscience XF^e96 Extracellular Flux Analyzer (Agilent) was used to monitor the mitochondrial oxygen consumption rate (OCR) and extracellular acidification rate (ECAR) in intact cells. The brain glial cells microglia, oligodendrocytes, and astrocytes) were seeded with a concentration of 50×10^4 cells per well in Poly-Lysine coated XF^e 96- well seahorse culture microplate in 100 μL of complete DMEM media and incubated overnight at 37°C in 5% CO_2 before the treatment. After 24hrs of indicated treatments, the growth media was aspirated, washed twice and replenished with 175 μL of pre-warmed bicarbonate-free DMEM (basal) assay media. The plate was incubated for 45 min at 37°C in a CO_2 free incubator for degassing. After incubation, OCR and ECAR were measured as per the manufacturer's protocol.

Early glycolytic ECAR estimation in microglia

The early glycolytic ECAR induction in microglia was measured using the XFe96 Extracellular Flux Analyzer after the cells were treated with LPS/IFNγ injection into a seahorse plate. During the degassing incubation period, the cells were pretreated with respective inhibitors (2DG, PDK1, and Akt) for 1 h. ECAR was measured as per the manufacturer's protocol.

Assessing metabolic fitness of microglia and O4 positive oligodendrocytes *in vivo* models using single-cell energetic metabolism by profiling translation inhibition (SCENITH)

We used the SCENITH assay, a method that allows for the analysis of the metabolic activities of particular cell populations, to check metabolic alterations in the Microglial and oligodendrocyte populations.[23] Utilizing this method, we conducted two different experimental methods to evaluate the metabolic activities of both cell populations such as endotoxemia and EAE. For endotoxemia, C57B6 mice were injected with LPS (1 mg/kg body weight) in the volume of 200 μL in PBS for 6hs before isolating brain. Second model, we used EAE in C57B6 induced by immunizing MOG_{35-55} in CFA.[71] Control group was injected with CFA alone. Post 18 days of immunization, brain, and spinal cord of EAE and CFA groups were harvested. Single cell suspension was prepared from brain of both *in vivo* models using Percoll gradient.[71] Single cell suspension was processed for SCENITH Assay. In brief, isolated cells were grouped into four different sets of conditions, and $1X\ 10^6$ cells were used for each treatment condition. The four treatment conditions include (i) control, (ii) 2-Deoxy-D-Glucose (2DG; final concentration 100 mM) treated, (iii) oligomycin (OM; final concentration 1 μM) treated and (iv) 2DGOM (2DG, first and then OM, combined) treated for 30mins. Each treatment group received Puromycin (Puro, 10 μg/mL; InvivoGen) during the final 15 min of the experiment. Metabolic inhibitor-containing media were discarded after the incubation period and washed with cold PBS. The cells were then stained using anti-Mouse CD16/32 for Fc receptor block (Biolegend), BV421-*anti*-CD45, BV510-*anti*-CD11b (for microglia populations; Biolegend), and anti-PE-O4 (for oligodendrocyte populations; Miltenyi Biotech) for 30 min at 4°C. Following incubations, cells were washed with FACS stain buffer, and fixed and permeabilized using Fixation/Permeabilization buffer set (Proteintech), as directed by the manufacturer instructions. Intracellular staining of Puro was performed using Anti-mouse AF647-Puro diluted (1:200) in permeabilization buffer for 1 h at room temperature. After incubation, cells were washed

3 times with FACS buffer and ran on Attune cytometry (ThermoFisher) and analyzed using FlowJo software. Using MFI of incorporated Puromycin, the mitochondrial dependence [100(control - OM)/control - 2DGOM)] and glucose dependence [100(control - 2DG)/control - 2DGOM)] were calculated.[23]

Western Blot analysis

After 24 h of treatment, the whole cells were extracted and washed with cold PBS and centrifuged. The pellet was lysed in protein lysis buffer (50 mm Tris-HCl, pH 7.4, containing 50 mm NaCl, 1 mm EDTA, 0.5 mm EGTA, 10% glycerol, and protease inhibitor mixture). The protein was estimated by Qubit fluorometric quantitation method (Thermo Scientific, Life technologies). Fifty micrograms of total protein lysate per lane were fractionated by 10% gradient SDS-PAGE and transferred to nitrocellulose membrane (Bio-Rad). Membranes were blocked in 5% nonfat dry milk (BioRad) in 0.1% TBS-T and incubated overnight with the indicated primary antibodies (1:1000) in 3% BSA-TBST at 4°C. After three consecutive washes with 0.1%TBST buffer, the blot was incubated with respective secondary antibody for 1h. Immunoreactivity was detected using enhanced chemiluminescence detection (Bio-Rad).

RNA extraction, cDNA synthesis and quantitative PCR

Total RNA was extracted using TRIzol and RNAeasy kit (Qiagen) as per the manufacturer's protocol. From the 1 μg of total RNA, cDNA was prepared using the iScript reversed transcriptase cDNA synthesis kit (BioRad). CFX96 Real-Time PCR Detection (Bio-Rad) was used to amplify all the genes. The primer sets and their nucleotide sequences were selected from the available online database and purchased from the Integrated DNA Technology (IDT Coralville, Iowa, USA) or ReaTimePrimers. The iTaq Univer SYBR Green Supermix was purchased from Bio-Rad. Thermal cycling amplification conditions were as follows: activation of DNA polymerase at 95°C for 3 min, followed by 40 cycles amplification at 95°C for 30 s and 60°C for 30 s. The expression of ribosomal protein L-27 housekeeping gene was used to calculate the normalized expression (^^Ct) of the target gene transcript using the CFX Maestro Software.

Immunocytochemistry (ICC)

Isolated oligodendrocytes were cultured on PLD-coated coverslips immersed in six-well plates. Once, the oligodendrocytes were differentiated ~70–80% confluence using T3 (30 nM) for 4 days, the microglial conditioned media (CM or CM-LI) was used to treat the cells. After 24 h of the treatment, the medium was aspirated, and coverslips were washed thrice with cold PBS and fixed with 4% paraformaldehyde for 15 min. The cells were washed with PBS, and 0.1% Saponin in PBS was added for 1 h. After PBS wash, the cells were blocked with 1% BSA in PBS for 30 min on a shaker at RT and incubated with primary antibody (diluted with 0.5%BSA) in 0.3% PBST for overnight at 4°C. The plate was washed thrice with PBS and incubated with appropriate secondary antibody for 1h at RT. DAPI (1: 10,000) was added for 10mins and cells were washed. After thorough washing, coverslips were mounted with mounting media on slides and image was captured using a fluorescence microscope.

Antisense experiment

To downregulate the expression of AKT and PDPK1 in primary microglia, the transfection media was prepared to a final volume of 100 μL/well with OptiMem containing siRNA (30 nm) for AKT or PDPK1 (Dharmacon) and Lipofectamine for the transfection experiment. Microglia were incubated for 6 h at 37°C and 5% CO2. The transfection media was replenished with complete media for 24 h after 6 h of transfection. The lentiviral silencing of iNOS was carried out according to the manufacturer's instructions (Santa Cruz Biotech). In brief, a complete media mixture containing 5 μg/ml Polybrene was prepared. After replacing the plate media with 1 mL of polybrene mixture media, cells were infected directly with shRNA Lentivirus particles and incubated overnight. The media was replaced with completely new media and left for another 24 h before being processed for the respective treatments.

Targeted metabolomics

Primary microglia were treated with LI as per experimental design and primary oligodendrocytes were treated with CM or CM-LI for 18 h, followed by washed three times with cold PBS and snap-frozen in liquid nitrogen. Metabolites were extracted with 80% methanol.[80] Approximately, one million (oligodendrocytes) or three million cells (primary microglia) were harvested and quenched before metabolite extraction using the following procedure. Cells were rapidly rinsed by gently dispensing 5 mL of 37°C deionized water to the cell surface. The plate was rocked briefly and aspirated and quenched by directly adding 10 mL of Liquid Nitrogen to the dish. A volume of 100 μL water (0.2% Formic acid) was added and vortexed to mix, and 10 μL of ISTD dilution mix was added. Subsequently, 400 μL of acetonitrile (0.2% formic acid) was added and vortex to mix. Three cycles of extraction were carried out by vertexing for 1 min followed by sonicating for 1 min (each). After this, the samples were centrifuged at 14,000 rpm for 15 min at 4°C. Supernatant were loaded into pre-conditioned Phenomenex, Strata XL-100, 30 mg/mL cartages and pass through it using positive pressure manifold. Subsequently, 50 μL of filtrate was mixed with 50 μL of water. 10 μL was injected into the LC-MS/MS system. Compounds were identified based on retention time and m/z match to injections of authentic standards. All TCA standards were reconstituted in (Water and Acetonitrile, 50:50) to prepare 10 mg/mL stock solutions. A standard curve at the range of 5–1000 ng/mL of each analyte (Citric acid, Aconitase, iso-citric acid, α-ketoglutaric acid, succinic acid, fumarate, malic acid and Oxoglutaric acid) was produced from stock solutions in the relevant matrix. 100 μL of each standard was mixed to obtain a mixed standard solution to further prepare a seven-point standard calibration curve within a range of 5–1000 ng/mL 10 μg/mL of each internal standard

(TCA-1 and TCA-2) were spiked into all samples as an internal standard (final concentration) to allow quantification based on the ratio of the internal standard to each intermediate peak (AUC). Phenomenex (Torrance, CA) Luna-NH2, 2.0 × 150 mm, 3 μm column was used to achieve an optimal separation of all TCA intermediates and to obtain good peak shapes. The flow rate of 0.3 mL/min was used with a mobile phase A (5 mM NH4OAc buffer at pH 9.9) and mobile phase B (Acetonitrile). Column temperature was optimized at 27°C for best peak shape. TCA cycle intermediates were monitored using MRM negative polarity. Identification was achieved based on retention time and product ions. Seven calibration standards ranging from 5 to 1000 ng/mL was subjected to the full extraction procedure three times before analysis. Mean correlation coefficients of each metabolite were linear $r^2 > 0.99$ were obtained (n = 3) from 5 to 1000 ng/mL. For stable isotope-resolved metabolomics (SIRM), primary oligodendrocytes treated with CM or CM-LI for 18 h were washed three times with warm glucose and serum free RPMI and plated cells in the same media with 10 mM of uniformly labeled [U-^{13}C]-Glc (glucose, Sigma) for 6 h. Cells were snap-frozen and metabolites were extracted with 80% methanol for measuring glycolytic/TCA metabolites enriched in ^{13}C derived from labeled glucose using LC/MS/MS.[81]

QUANTIFICATION AND STATISTICAL ANALYSIS

Data were analyzed and plotted using Microsoft Excel and/or GraphPad Prism (Version 9.0.0) softwares. Statistical analysis of data related to OCR, ECAR, ATP, Real-time PCR and immunoblot was performed using Student's *t* test for two group comparison and data were presented as mean ± SD from three different sets of the experiment. p values < 0.05 was considered significant.